A KINETIC STUDY OF MONOMER-POLYMER RATIO AND MOLECULAR WEIGHT DEVELOPMENT IN IDEAL STYRENE EMULSION POLYMERIZATION

by

MICHAEL R. GRANCIO

A dissertation submitted to the Graduate Faculty in Engineering in partial fulfillment of the requirements for the degree of Doctor of Philosophy, The City University of New York.

1969

This manuscript has been read and accepted for the Graduate Faculty in Engineering in satisfaction of the dissertation requirement for the degree of Doctor of Philosophy.

May 7, 1969
date

David J. Williams
Chairman of Examining Committee

7 May 1969
date

Executive Officer

Dr. Stanley Katz

Dr. Herbert Meislich

Dr. Reuel Shinnar

Dr. Arthur E. Woodward

Dr. David J. Williams, Chairman

Supervisory Committee

The City University of New York

Abstract

This study presents a heterogeneous monomer-polymer particle model for the emulsion polymerization of styrene. The possibility of such a model is strongly suggested by accumulated kinetic data, and the existence of the model is verified by a direct experiment involving the slicing and viewing of a single latex particle.

Continuously uniform latices are applied to an experimental kinetic study of molecular weight and monomer-polymer ratio development in ideal styrene emulsion polymerization. The time dependent polymerization parameters of conversion rate, particle size, monomer-polymer ratio, molecular weight, and radical generation are directly followed for a classical type styrene system. New experimental techniques generally applicable to emulsion polymerization are presented; these include single charge generation of continuously uniform latices, dynamic measurement of monomer-polymer ratios, the extension of inhibitor studies in emulsion polymerization and the use of electron microscopy to directly examine latex particle morphology.

Experiments center around a single formulation with the following characteristics: a constant rate of 13% conversion per hour up to 60%, a final uniform particle diameter of 2,300 A, pH = 9 (constant), and approximately 10^{14} particles per ml.

The kinetic data for this system show: (1) As is commonly observed, the number of particles remains constant, and the number of free radicals per particle equals ½ during the constant rate period. (2) In contrast to conclusions drawn from equilibrium swelling measurements, but in agreement with the original work of Harkins, the monomer-polymer ratio is continuously changing throughout the reaction. (3) In situ inhibitor perturbation studies conclusively show that $K_2S_2O_8$ decomposition is first order with 100% efficient generation of free radicals. (4) In contrast to the prediction of current steady state theory the instantaneous number and viscosity average molecular weights increase 5-6 fold to their maximum values during the constant rate period. These kinetic results suggest a heterogeneous model for the monomer-polymer particle wherein polymerization takes place in a monomer rich zone surrounding a growing polymer core. Direct electron microscopic observation of the cross section of a monomer-polymer particle verifies the model suggested by the kinetic approach.

Acknowledgements

The author is greatly indebted to Dr. David J. Williams for his guidance and continual interest in this research. The author expresses thanks to Dr. A.E. Hamielec for running gel permeation chromatography samples and Mr. Mark Roller for his assistance in the development of gas chromatography techniques. The major portion of this work was supported by the National Science Foundation under grant GK 1375.

Table of Contents

List of Tables

List of Figures

I - Introduction

The currently accepted mechanism of emulsion polymerization is described both qualitatively (1) and quantitatively (2, 3, 4) in the literature. While numerous experimental studies have been conducted in attempts to verify this mechanism and the associated theories (5-10), most of these have neglected the development of the monomer-polymer ratio and molecular weight during the course of a run. Further, it has generally been assumed that the monomer-polymer particle is homogeneous. Briefly, theory requires that the monomer-polymer ratio should remain constant (1) with monomer uniformly distributed throughout the particle and predicts that a constant molecular weight should be generated during the constant rate period (6, 11, 12). There is limited evidence, however, that the monomer-polymer ratio actually changes continuously throughout the entire reaction (1). Also, a several fold increase in molecular weight has been observed during the constant rate period of a "typical" emulsion polymerization (6, 11, 12).

Advanced analytic treatments (3, 4) are based on the solution of the Smith-Ewart recursion formula (2) for a homogeneous monomer-polymer particle. These predict an increasing molecular weight only for the non-ideal case of increasing radical concentration, and therefore increasing polymerization rate, within a particle (3) or for initiator kinetics which are not applicable to the systems being

studied (13). When extrapolated to the limiting conditions of ideal* emulsion polymerization these treatments predict a time constant molecular weight.

Most experimental kinetic studies have tended to emphasize a limited number of reaction variables (7, 8, 15). Thus, there is not sufficient data for any particular system to extract a mechanism for increasing molecular weight. In addition, monomer-polymer ratio measurements have been restricted to equilibrium swelling conditions (12) rather than dynamic studies.

This dissertation centers around a clarification of molecular weight and monomer-polymer ratio development during ideal emulsion polymerization as well as an elucidation of the morphology of the monomer-polymer particle. The practice of utilizing continuously uniform latices (11, 16) is continued and extended, since it was shown that these latices can be of considerable value in such studies (11). Number average and viscosity average molecular weights were followed during the course of a run to indicate the magnitude of their increase and to clarify the earlier data of Smith (6) and Williams and Bobalek (11).

*Ideal emulsion polymerization has been defined by Van der Hoff (14) as emulsion polymerization occurring at a constant conversion rate with the average number of radicals in a particle, $\bar{n}$, being constant and equal to $\frac{1}{2}$.

For this same run, conversion rate, detailed initiator kinetics, dynamic (rather than equilibrium) monomer-polymer ratio, particle growth, and molecular weight distribution were also followed with time. This represents the most comprehensive set of data yet obtained for one system in emulsion polymerization.

During the course of the work, several new experimental techniques were developed to obtain the data. These are generally applicable to emulsion polymerization and include a method for single charge generation of continuously uniform latices, measurement of dynamic monomer-polymer ratios, certain free radical generation rate measurements, and the use of electron microscopy to directly examine particle morphology.

The kinetic data so accumulated helped to clarify the scope of the problem, eliminated certain mechanisms for the observed molecular weight increase during the ideal period and strongly suggested others. Interpretation of these data suggested a heterogeneous monomer-polymer particle which was later confirmed by direct electron microscope observation of a single particle cross section.

II - Historical Background

A. Qualitative Theory

The basic ingredients in a classical type emulsion polymerization formulation are, on a parts by weight basis, 180 parts water, 100 parts of a very slightly water soluble vinyl monomer, 3-5 parts soap, and 0.5 parts of a water soluble initiator. The presently accepted qualitative description for the emulsion polymerization system of interest was first advanced by Harkins (1).

Briefly, Harkins pictured emulsion polymerization as a three stage process occurring in a homogeneous environment. In the first stage, monomer-polymer particles are generated from soap micelles which have been activated by free radicals entering from the aqueous phase. Monomer continuously diffuses into the monomer-polymer particles to sustain growth while soap from the unactivated micelles migrates to the particle surfaces to stabilize them. The nucleation stage ends at about 10% conversion when all of the micellar soap disappears.

At this point the second stage begins. Three separate phases exist during this stage. The monomer-polymer particles continue to grow while monomer is continuously supplied from the emulsified monomer phase and initiator enters from the aqueous phase. The second stage often exhibits constant-rate behavior. This is the major growth stage and therefore the region of major concern in this

study. Stage 2 ends at about 60% conversion when all of the monomer has diffused into the particles. The third stage in emulsion polymerization involves reaction of the remaining monomer in the monomer-polymer particle.

This description of emulsion polymerization has changed little since its conception. The more recent literature (17), however, challenges the role of soap micelles in particle nucleation. This challenge arises primarily from the fact that particles can be nucleated in systems whose soap concentration is below the critical micellar concentration.

B - Quantitative Theory

1 - Smith-Ewart Theory

The quantitative aspects of emulsion polymerization were first considered by Smith and Ewart in 1948 (2). Their theory provided the major impetus to most subsequent emulsion polymerization research. For that reason we will discuss the Smith-Ewart theory in some detail.

Smith and Ewart were primarily concerned with developing equations for the number of particles formed in an emulsion polymerization system and for the consequent rate of polymerization. In their treatment, they considered the monomer-polymer particles as isolated, homogeneous loci of polymerization with free radicals entering from an external medium, the aqueous phase.

Consider a system consisting of 1cc of external medium having suspended in it N isolated reaction loci (monomer-polymer particles) each of volume v and surface a. If free radicals are generated externally the rate at which free radicals enter a particle is given by:

$$\frac{dn}{dt} = p'/N$$

where p' is the rate at which radicals enter all particles.

The rate at which free radicals may escape a particle is expressed as:

$$\frac{dn}{dt} = -k_o a \left(\frac{n}{v}\right)$$

where k_o is a specific rate constant and $\left(\frac{n}{V}\right)$ is the concentration of free radicals within the particle.

Further, suppose that destruction of free radicals occurs only by mutual termination. Then, the rate of radical destruction within the particle is given by:

$$\frac{dn}{dt} = -2k_t\, n\left[\frac{n-1}{v}\right]$$

where $[n-1]/v$ is the concentration of free radicals with which any of the n free radicals in a locus can react; k_t is a specific rate constant, and the constant, two, results from the hypothesis of mutual termination.

If these three events are the only ones which need be considered in determining the numbers of free radicals in the various reaction loci, then the N_o, N_1, $N_2 \ldots N_n \ldots$ reaction loci respectively containing 0, 1, 2, ...n..... free radicals will be related by the steady state condition:

$$N_{n-1}\left(\frac{p'}{N}\right) + N_{n+1}k_o a\left[\frac{n+1}{V}\right] + N_{n+2}k_t\left[(n+2)\left(\frac{n+1}{V}\right)\right]$$

$$= N_n\left[\left(\frac{p'}{N}\right) + k_o a\left(\frac{n}{V}\right) + k_t\, n\left(\frac{n-1}{V}\right)\right]$$

This is the Smith-Ewart recursion formula which states that the rate of formation of reaction loci characterized by containing n free radicals is equal to the rate of disappearance of these loci.

Smith and Ewart solved this equation only for the three special cases of $\bar{n}<<<1$ (Case I), $\bar{n} = \frac{1}{2}$ (Case II), and $\bar{n}>>>1$ (Case III), where $\bar{n}$ is the average number of radicals

in a particle. They considered Case II of special interest in that it best explains the unique nature of emulsion polymerization.

The assumptions involved in the Case II solution are that no radicals escape from the particles and that mutual termination of radicals within the particle is almost instantaneous. This can be expressed as:

$$(1)\quad k_o\left(\frac{a}{v}\right) \ll p'/N \ll \frac{k_t}{v}$$

Discarding terms in k_o the recursion formula may be rewritten as:

$$N_{n-1} + N_{n+2}\, B(n+2)(n+1) = N_n\,[1+Bn(n-1)]$$

where $$B = \frac{k_t N}{v p'}$$

Smith and Ewart further show that for B>1 (assumed in equation (1)) the recursion formula can be approximated by:

$$(2)\quad \frac{N_{n-1}}{N_n} = 1 + Bn(n-1)$$

The total number of radicals in the system will be:

$$(3)\quad n_T = N_1 + 2N_2 + 3N_3 + \cdots\cdots\cdots$$

The total number of particles in the system will be:

$$(4)\quad N = N_o + N_1 + N_2 + \cdots\cdots\cdots$$

Combining equations (2), (3) and (4) the total number of radicals in the system is seen to be:

$$(5)\quad n_T = \frac{N}{2}\left[1 + 1/B + \frac{1}{3B^2} + \ldots\ldots\right]$$

If $B \gg 1$ then $n_T = N/2$ or $\bar{n} = \frac{1}{2}$. For this case the rate of polymerization is given by:

$$(6)\quad \frac{dM}{dt} = k_p[M]\, N/2$$

where t is time and [M] is the monomer concentration. The average lifetime of a radical within a particle is given by:

$$(7)\quad \bar{\tau}_p = N/2p'$$

Thus, as the number of particles is increased both the rate and the average radical lifetime or molecular weight increase. This simultaneous increase in rate and molecular weight is a unique feature of emulsion polymerization and is attributable to isolated growth of radicals within the monomer-polymer particles. $\bar{n} = \frac{1}{2}$ implies a zero-one model wherein the nth radical enters a particle and polymerizes undisturbed until the n+1th radical enters the particle to terminate it instantaneously. The particle then lies dormant until the n+2th radical enters the particle. Equations pertaining to the number of particles generated are not especially cogent to the present work and will therefore be omitted.

2 - Medvedev Theory

Most other quantitative treatments of emulsion polymerization build on the Smith-Ewart theory. The only radically different approach was presented by Medvedev (18). Medvedev postulated that as polymerization progressed the internal viscosity of the particle became such that free radicals could not penetrate the particle. He thus suggested that free radicals being unable to penetrate the particle reacted with emulsifier molecules and that these emulsifier radicals in turn reacted with monomer at the surface of the particle. There is some support (7) and some refutation (16) of the Medvedev theory in the literature, but for the most part the Medvedev approach is ignored. This is mainly because Medvedev's postulate of constant monomer-polymer particle surface area during the course of reaction is inconsistent with reality.

3 - Extensions of Smith-Ewart Theory

In 1957 Stockmayer presented a general solution to the Smith-Ewart recursion formula (3). Stockmayer solved for the average number of radicals per particle in terms of two parameters:

$$m = \frac{k_o a}{k_t} \quad ; \quad b = \left[\frac{8v}{k_t \bar{t}_p}\right]^{\frac{1}{2}}$$

where the nomenclature follows that of Smith and Ewart presented above. Stockmayer's solution is presented in graphical form as Figure 1.

In 1965 O'Toole (4) showed that although Stockmayer's solution was mathematically correct it did not hold for systems which have a finite rate of radical desorption. O'Toole's modifications of the Stockmayer solution are shown as dotted lines in Figure 1. Since the Stockmayer and O'Toole treatments are basically for non-ideal emulsion polymerization they will not be considered in any further detail.

The above treatments represent the best analytic approach to emulsion polymerization to date. More recent analytic papers have combined kinetics and probability with the Smith-Ewart theory to develop expressions for molecular weight distribution development as well as other important polymerization parameters (12, 13, 19-23). It is important to note especially, however, that all have considered the monomer-polymer particle to be homogeneous.

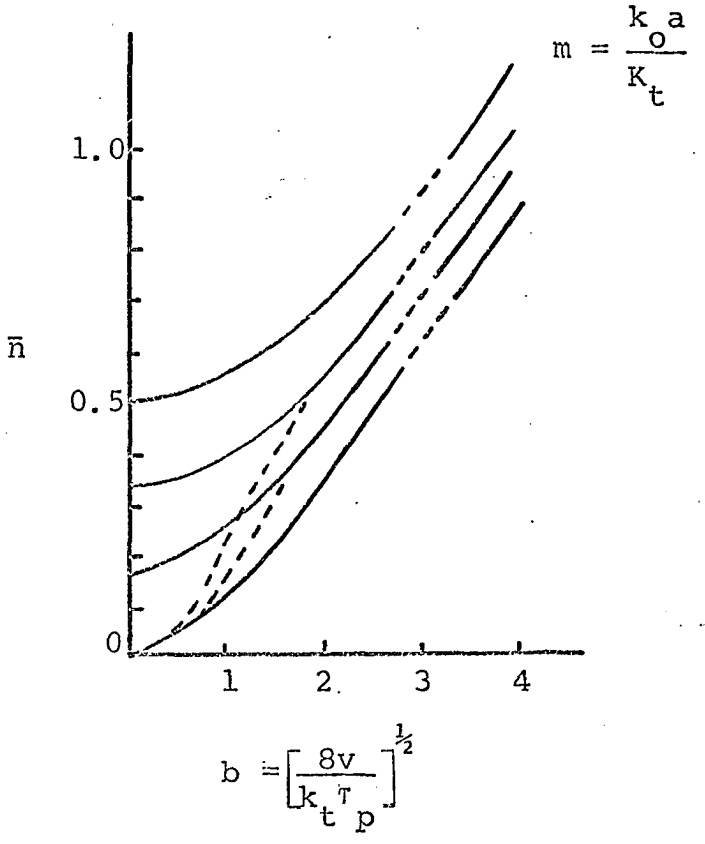

FIGURE I. AVERAGE NUMBER OF RADICALS PER PARTICLE, $\bar{n}$
STOCKMAYER (——); OTOOLE (---)

4 - Experimental Verification of Smith-Ewart Theory

The Smith-Ewart theory has generated virtually innumerable experimental studies. Most studies, however, have not been explicit in their kinetic approach. Many researchers have concerned themselves with the relationship between the number of particles formed and the initial concentration of soap and initiator (7, 14). Still others have dealt with the effect of particle size, particle number and initiator concentration on the rate of polymerization (2, 9, 10, 12, 19-23). Most of these studies purport to verify the Smith-Ewart theory as it stands with the Stockmayer solution. There are, however, two important emulsion polymerization parameters, monomer-polymer ratio and molecular weight development, whose relationship to Smith-Ewart theory has not yet been fully elucidated. These parameters will be discussed in detail below.

5 - Monomer-Polymer Ratio

Consider the monomer-polymer ratio. It has been shown above that for Smith-Ewart Case II, $\bar{n} = \frac{1}{2}$, the rate of polymerization can be expressed as:

$$(6) \qquad R_p = k_p [M]^{N/2}$$

Many systems exhibit a constant rate of polymerization with $\bar{n} = \frac{1}{2}$ and constant during stage II of emulsion polymerization between about 10 and 60 percent conversion. For this

reason Stage II has been called the "ideal period" (14). Since k_p and N/2 are constant, a constant rate during the ideal period implies a constant monomer-polymer ratio in accordance with theory as expressed in equation (6).

Harkins' early experiments, however, indicated that the monomer-polymer ratio decreased as much as three-fold between 5 and 50 percent conversion (1, 24). Harkins determined the monomer-polymer ratio by centrifuging a reaction sample for three minutes at 5,000 gms. and measuring the resultant styrene layer. Comparison of the amount of styrene layer and conversion yielded the monomer-polymer ratio. This was an approximate dynamic measurement. Outside of the original paper and a mention in Bovey's text (25) this pertinent work has been ignored in the literature.

Subsequently, workers have confined their studies to measurement of equilibrium monomer-polymer ratios (5, 15, 27). This involves taking a latex of known particle diameter, diluting it to about 10% solids with soap solution and swelling it with monomer (15). The monomer-polymer ratio is determined from the quantity of monomer absorbed by the particles. This is obviously an inferior method of determination in that the equilibrium ratio is not necessarily the one that maintains during the actual reaction. This can readily be seen from the fact that it takes anywhere between 20 minutes and 5 hours to swell a particle in which no reaction is occurring (5, 15). For example, for the system of interest in this thesis it would take between one and two hours to swell the final latex.

Using the equilibrium technique Smith found that the monomer-polymer ratio is a slightly increasing function of particle diameter (5). Thus, he maintained that if anything the monomer-polymer ratio should increase slightly in the course of reaction. This postulate was supported by Meehan who found that the equilibrium monomer-polyer ratio was a slightly increasing function of particle diameter but not a function of molecular weight or soap concentration (26). Morton et al. agreed that the monomer-polymer ratio was to some extent dependent upon particle diameter and independent of molecular weight, but they found a dependence upon soap concentration that was reflected in surface tension changes (15). All of these workers, however, concurred that the dependence of the equilibrium monomer-polymer ratio on diameter was small enough so that the ratio could be considered constant for the change in diameter normally observed during the ideal period.

Smith (5) suggested that this constancy of monomer-polymer ratio results from a balance between the effect of monomer activity in the monomer-polymer solution and the effect of interfacial tension of the very small particles. This equilibrium was expressed quantitatively by Morton et al. (15). They combined an expression for the interfacial free energy of the particle with the Flory-Huggins equation for the activity of monomer in the monomer-polymer particle to obtain:

$$(8)\quad -\left[\ln (1-v_2) + v_2 + \mu v_2^2\right] = \frac{2V_1\gamma}{rRT}$$

where:

v_2 = volume fraction of polymer in the particle

μ = polymer-monomer interaction parameter

V_1 = molar volume of the monomer

γ = interfacial tension between the particle and water

r = radius of the particle

In the most recent literature reviews (14, 12, 19-23), the constant rate or ideal period in emulsion polymerization has been explained by equation (6) assuming that the monomer-polymer ratio is essentially constant. Although this may be true for some systems, it is still open to question as a general statement. In the first place, there is the consideration of whether or not an equilibrium measurement can be extrapolated to kinetic conditions. Again, there is the question of conflicting trends reported in the literature as discussed above. Finally, even small increases in monomer-polymer ratios during the ideal period should be reflected in increased conversion rates. For many systems, this increased rate is not observed. The dynamic monomer-polymer ratio in the course of reaction will be an important consideration in this thesis.

As discussed above, the monomer-polymer ratio is dependent upon the thermodynamic conditions of the monomer-polymer particles and their environment. It should be men-

tioned at this time, however, that one must be careful in applying classical thermodynamics to the monomer-polymer particle. Consider a monomer-polymer particle 2000 A in diameter containing polymer of average molecular weight 500,000. In this case the fully extended chain length of each polymer molecule is about six times greater than the diameter of the particle, and the radius of gyration of the molecule (in a good solvent) is about 1/6th the particle diameter (31). Thus, the elements of the monomer-polymer particle (the polymer molecules) are on the same order of size as the particle itself. Further, each chain grows independently in an isolated reactor, and at 100% conversion each particle will contain less than 10,000 polymer chains. This is not a statistical number of molecules. The applicability of classical thermodynamics under these conditions is questionable.

6 - Molecular Weight Development

A second important emulsion polymerization parameter which is yet to be described theoretically is molecular weight development during the ideal period. To begin, consider the instantaneous number average degree of polymerization predicted by steady state theory, termination by combination:

$$(9) \quad \bar{x}_{nip} = \frac{2R_{pp}}{R_{tp}} = \frac{2R_{pp}}{R_{ip}}$$

where: $\bar{x}_{nip}$ = the particle instantaneous number average degree of polymerization.

R_{pp} = the rate of polymerization per particle, moles/l. sec.

R_{tp} = the rate of termination of polymer chains within the particle moles/l.sec.

R_{ip} = the rate of initiation of polymer chains within the particle, $\frac{\text{moles}}{\text{l.sec.}}$

Steady state theory dictates that $R_{tp} = R_{ip}$.

It has been established that potassium persulfate, the usual initiator in emulsion polymerization decomposes in aqueous solution by first order kinetics as: (28)

$$(10) \quad \frac{d[I]}{dt} = 2k_D[I]$$

where: $[I]$ = initiator concentration, $\frac{\text{moles}}{\text{l.}}$

k_D = specific decomposition rate constant sec.^{-1}

t = time

If equation (10) is integrated and 100% radical efficiency is assumed then:

$$(11) \quad R_{ip} = 2k_D[I_o]\, e^{-k_D t}$$

where: $[I_o]$ = the initial initiator concentration; $\frac{\text{moles}}{\ell.}$

t = reaction time, sec.

Combining equations (9) and (11).

$$(12) \quad \bar{x}_{nip} = \frac{R_{pp}}{k_D[I_o]}\, e^{k_D t}$$

Equation (12) represents the predicted steady state instantaneous number average degree of polymerization. The decomposition constant, k_D, as measured by Kolthoff et al. (28) was found to be on the order of 10^{-4} min.$^{-1}$. For this low value of k_D the exponential term in equation (12) can be assumed to be almost unity throughout the course of reaction. Thus, since k_D and $[I_o]$ are constants, equation (12) predicts a constant instantaneous number average molecular weight during the ideal period when R_{pp} is constant. Previous investigators (14, 21) have assumed the pure aqueous decomposition kinetics of Kolthoff (8, 11, 12, 28) in predicting molecular weights. This is not strictly valid in view of the fact that several studies have shown that persulfate decomposes as much as eight times faster in the presence of soaps (29, 30). Up to now initiator kinetics have not been followed throughout the course of reaction in the actual polymerization medium. This dissertation will include such data.

Most kinetic studies of emulsion polymerization have neglected molecular weight development so that data of this sort are scanty in the literature. Most of those who have measured molecular weights have chosen to measure only final molecular weights (14, 9, 10). Thus, they characterize the entire reaction by the molecular weight of the final product. For example, van der Hoff uses final molecular weights in conjunction with Kolthoff's decomposition data to calculate radical efficiencies of 0.2 to 0.6 (29). Gerrens (9, 10), and Gardon (19, 12) make similar use of final molecular weights. Kolthoff on the other hand uses final molecular weights to count the average number of persulfate groups per chain (30).

There have, however, been three studies of molecular weight development in persulfate initiated styrene emulsion polymerization. Each of these studies (5, 11, 12) indicates a substantial increase in molecular weight during the second stage of emulsion polymerization. This is in direct conflict with steady state theory as presented in equation (12). The molecular weight data of Williams for example shows up to 500% increase during the ideal period.

Williams and Bobalek (11) presented their data as an indication of discrepancy between observation and steady state theory. Gardon (12), on the other hand, attempted to reconcile his data to the Smith-Ewart theory. Gardon's reasoning was as follows: Consider Stockmayer's solution to the Smith-Ewart recursion formula as presented in Figure 1. As the volume of the particle, v, increases

(if k_t is finite) "b" increases and therefore $\bar{n}$ increases. Physically what this means is that if k_t is finite, as the particle volume increases it will take a succeedingly longer time for two radicals to find each other and terminate. Thus, the average lifetime of a radical increases. Subsequently, the molecular weight increases with particle volume.

We will now digress to present Gerrens' very simple but interesting mathematical expression for this same phenomenon (9). Consider the nth radical entering a particle. It will grow undisturbed for some time t which is the time between successive entry of two radicals. At time t the n+1th radical will enter the particle. It will take some finite time Δt for the two radicals to meet and terminate. Then there will be a time interval $t-\Delta t$ until the n+2th radical enters the particle to reinitiate polymerization. The average number of radicals in a particle over time interval 2t will be:

$$(13) \quad \bar{n} = \frac{t + 2\Delta t}{2t} = \tfrac{1}{2} + {}^{\Delta t}/_{t}$$

If k_t is finite, as the volume of the particle increases Δt and therefore $\bar{n}$ increases.

This argument presents a valid explanation for molecular weight increase in emulsion polymerization, but it is questionable as a general statement on two accounts. First, an increase in $\bar{n}$ also predicts an increase in the rate of polymerization. Although some of Gardon's data

show conversion curves which are slightly convex to the time axis we would expect a much greater increase in conversion rate for a change in $\bar{n}$ concomitant with the observed increase in molecular weight. Secondly, Gardon illustrates a finite termination time by means of post add initiator techniques. He reports [after Gerrens (9)] an increase in conversion rate following addition of initiator to a run in progress. This is support for his model. Williams, however, reports large increases in molecular weight for systems which do not exhibit increased rates with post added initiator (11, 16). In Williams' work, he doubled and tripled initiator concentration without changing the rate of conversion. Similar data will be presented later in the present study.

To summarize, Gardon's explanation for molecular weight increase in emulsion polymerization may be valid for the non-ideal case of increasing $\bar{n}$; however, his own rate data do not increase as much as they should based on such an explanation. Further, Williams and Bobalek have shown molecular weight increase in the ideal case of $\bar{n} = \frac{1}{2}$ and constant.

The above authors have presented their data as cumulative viscosity average molecular weights. Brief reflection will reveal that the instantaneous molecular weight increases even more dramatically. This point will be considered later in greater detail. Again, in order to compare experimental molecular weights to the theoretical equation (12) we should also have a measure of the

number average molecular weight. Number average molecular weights, unlike viscosity averages, are free from the influence of branching or transfer to monomers. Thus, direct measurement of number average molecular weights should provide a clearer understanding of any discrepancy between what is observed and predicted. This dissertation reports the first measurement of number average molecular weight during the course of reaction.

7 - Continuously Uniform Latices

Except for the work of Williams and Bobalek (11, 16), the experiments discussed above were carried out in polydisperse systems. The distribution of particle sizes injects one more obfuscating variable into the system and concentrates attention on the bulk. The use of continuously uniform latices, however, focuses attention on the monomer-polymer particle which is the actual locus of reaction and eliminates particle nucleation rate as a variable in the first stage.

The basic theory behind the generation of continuously uniform latices is clearly outlined by Bobalek et al. (32, 33). Briefly, the generation of such latices involves initial soap starvation so that particle nucleation occurs all at once. Additional soap is usually added slowly as the reaction proceeds to stabilize the growing monomer-polymer particles without nucleating new particles.

Williams (11, 16) suggested that continuously uniform latices could be used to make the monomer-polymer particle more analytically accessible. He pointed out that a dynamic equivalence will exist between the identically sized particles so that the particles could be considered uniform in every respect. The molecular weight development of the polymer generated in any particle can be considered the same as the molecular weight measured for the bulk. Again, any particle rate process is simply the overall bulk rate divided by the number of particles. Thus,

attention is focused on the monomer-polymer particle as the actual locus of polymerization.

Williams (11) also showed that continuously uniform latices are suitable for kinetic studies of emulsion polymerization in that they are kinetically similar to their polydisperse counterparts. That is, the rate and molecular weight curves, particle sizes and numbers of particles formed are identical for both polydisperse and continuously uniform systems.

III - Current Research

A - Introduction

As previously indicated, current steady state theory does not explain the increase in molecular weight observed during the ideal period of emulsion polymerization. According to the current literature, the problem is not clearly defined. In fact, many researchers ignore the fact that a discrepancy in theory exists. Thus, the first purpose of this dissertation is to define the scope of the problem. A second important consideration in this work is the development of the dynamic monomer-polymer ratio. This heretofore neglected variable provides new insight into the kinetic mechanism of emulsion polymerization and the morphology of the monomer-polymer particle.

The work herein described is based on experimental research. Attention is focused primarily on one system which is similar to other systems (11, 16) exhibiting ideal emulsion polymerization. It is important to note that the formulation used generates continuously uniform latices. This allows us to focus on the monomer-polymer particle as the actual locus of polymerization. The data presented here represent the most extensive and complete set of data yet published for a single emulsion polymerization system. Several reaction parameters, namely: conversion rate, particle size, dynamic monomer-polymer ratio, free radical generation and molecular weight development, are simultaneously followed with time. The purpose of this approach has been

to collect sufficient data for one system so as to isolate a plausible mechanism for increasing molecular weight during the ideal period of emulsion polymerization. The data, conclusions and model developed are presented as a basis for further study.

The data are presented and discussed in this section. In order to lend continuity and clarity to its development, detailed discussion of the experimental work and new experimental techniques has been located in the Appendix. Such discussion is held to a minimum here but in the Appendix the reader should note the discussion on monomer-polymer ratio, inhibitor, and the electron microscope morphological studies which represent new experimental techniques.

B - Polymerization

The polymerizations were conducted in both a bottle polymerizer and a paddle mixed, one liter reactor. Both reactors were maintained at 60±1°C. The kettle reactor was fitted with a thermometer, condenser, and a glass tube device for purging and sampling. In both reactors the entire formulation, except for the initiator, was charged initially. After a period of nitrogen purging, the persulfate was added in solution form. Standard techniques were used for the purification of monomer.

A bottle run consisted of several simultaneously charged identical bottles. This method was employed, especially at low conversions, when it was desired to obtain sufficiently large polymer samples. Runs labelled KI, KII were performed in a kettle; runs labelled BI, BII, BIII were performed in bottles.

C - Formulation and Particle Size

It was desired to develop a suitable formulation to study molecular weight development in ideal emulsion polymerization. The system, in addition to being kinetically equivalent to its classical polydisperse counterparts, had to meet the following criteria: (1) exhibit constant rate behavior with $\bar{n} = \frac{1}{2}$ over a wide range of conversion, (2) generate continuously uniform latices, (3) be stable throughout a run under varying agitation rates, (4) generate a maximum number average molecular weight of 10^6 (the maximum measurable), (5) transpire in a reasonable time, and (6) all of the initiator had to decompose to free radicals (pH>7) (28) to eliminate the possibility of side reactions. The formulation finally developed consisted of: 180 g. water, 100 g. styrene, 0.15 g. sodium lauryl sulfate, 3.00 g. Triton X-100, 0.075 g. KOH and 0.500 g. $K_2S_2O_8$. The formulation was characterized by: 13% conversion per hour, a final particle diameter of 2,300Å, pH = 9, and approximately 10^{14} particles per ml. Unless otherwise stated the data presented in this section are for this standard formulation.

In addition to fulfilling the above requirements, this formulation proved to be advantageous in that it could be manipulated as a single charge. Previous uniform latex formulations suitable for these kinetic studies involved slow soap addition techniques which were tedious. It is felt that this specific formulation is successful

because Triton X-100 is a poor particle nucleator (34). Thus the small amount of sodium lauryl sulfate provides the "soap-starved" environment necessary to generate continuously uniform latices while the Triton X-100 provides the surfactant necessary for particle stabilization.

Electron micrographs of latices at progressive stages of growth are shown in Figures 2-5. Two sizes of particles are seen: the larger are calibration standards while the smaller are the actual samples. As can be seen from these micrographs and the uniformity count data in Table 1, these latices are remarkably uniform throughout the course of reaction. Uniformity ratios are reported as the ratio of weight average to number average particle diameters. Standard electron microscopy techniques were employed (35) with a Norelco EM 300 electron microscope.

The fact that this formulation leads to a system that is kinetically equivalent to its polydisperse counterparts is easily verified. Consideration of the data to be presented will show that conversion and molecular weight curves, particle numbers and particle diameters for this system are on the same order as those observed in polydisperse latices (11).

TABLE I

PARTICLE UNIFORMITY

SAMPLE	% CONVERSION (GRAVIMETRIC)	NUMBER OF PARTICLES COUNTED	PARTICLE DIAMETER Å	UNIFORMITY RATIO	% CONVERSION (FROM D_p)
KI-1	8%	14	1,025	< 1.01	8.8%
KII-2	22%	30	1,390	< 1.01	22.0%
BI-6	42%	20	1,740	< 1.01	43.2%
KI-4	76%	40	2,100	1.01	76.2%
BI-10	100%	40	2,300	< 1.001	100%

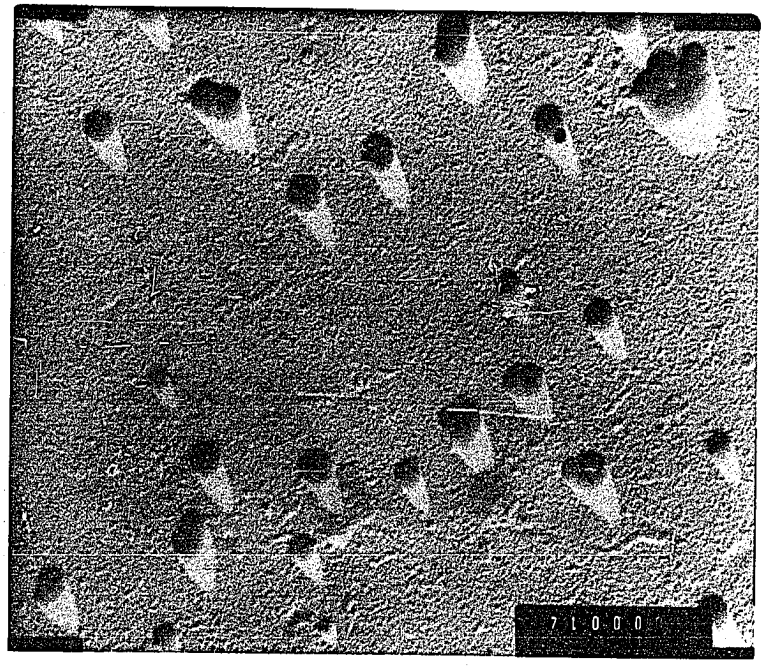

FIGURE 2: SAMPLE KII-1 (PLATINUM SHADOWED) 8% CONVERSION PARTICLE DIAMETER 1,025Å; STANDARD DIAMETER 1,305Å, ELECTRONIC MAGNIFICATION 28,000x

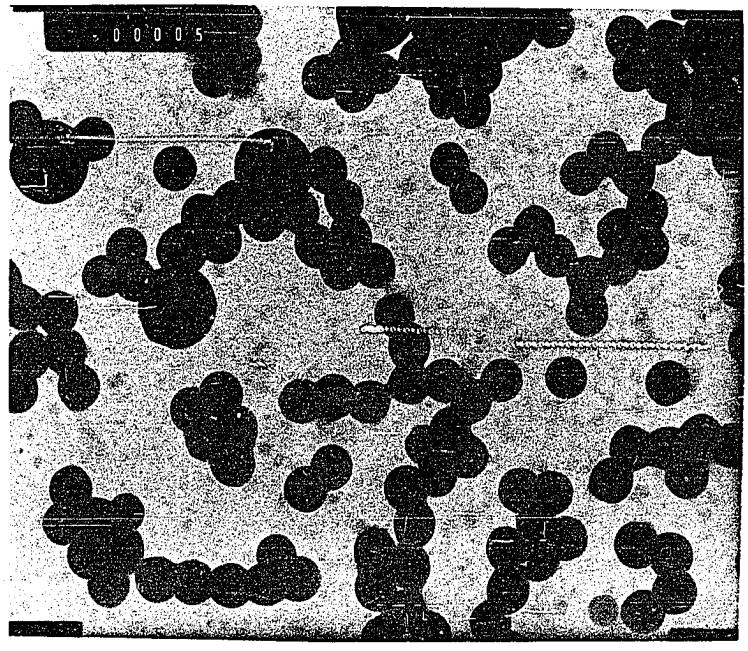

FIGURE 3: SAMPLE KII-2 (UNSHADOWED)
22% CONVERSION: PARTICLE DIAMETER 1,390Å
STANDARD DIAMETER 2,640Å
ELECTRONIC MAGNIFICATION 35,000x

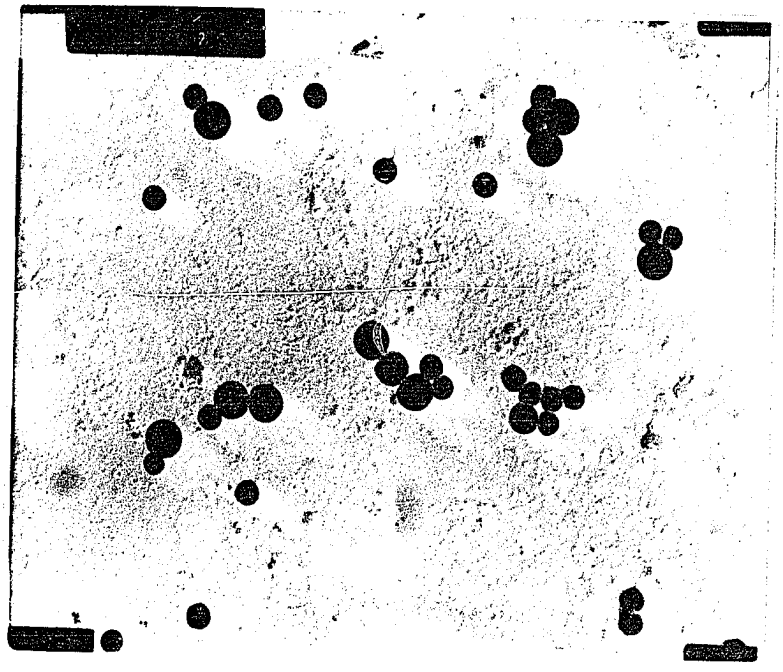

FIGURE 4: SAMPLE BI-6 (PLATINUM SHADOWED)
42% CONVERSION; PARTICLE DIAMETER 1,740Å
STANDARD DIAMETER 2,640Å
ELECTRONIC MAGNIFICATION 18,000x

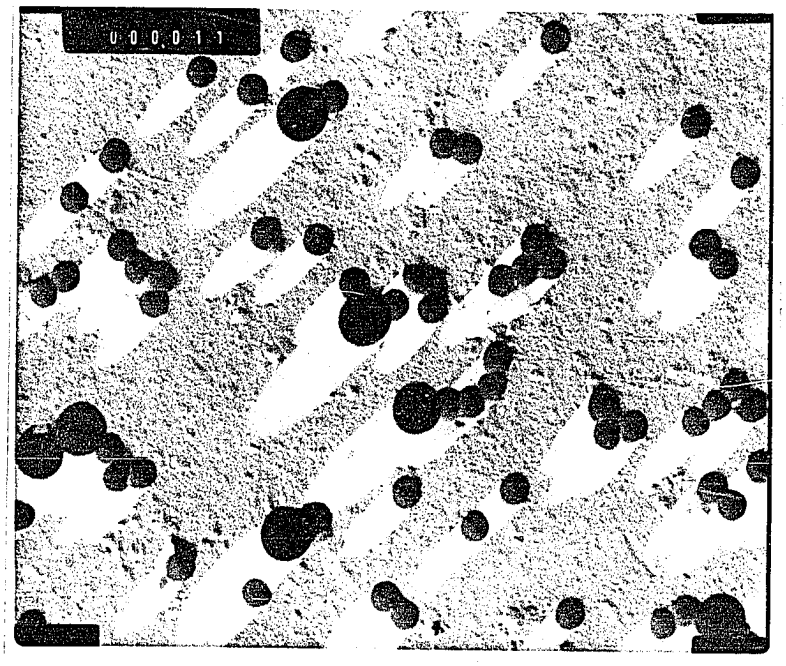

FIGURE 5: SAMPLE BI-10 (PLATINUM SHADOWED)
100% CONVERSION; PARTICLE DIAMETER 2,300Å
STANDARD DIAMETER 3,650Å
ELECTRONIC MAGNIFICATION 18,000x

D - Conversion Rate

Since the latices were continuously uniform the extent of reaction could be determined in two ways: (1) by taking the ratio of the cubes of the intermediate to final particle diameters and (2) by gravimetric means. As shown in Table 1, both methods give the same results within the limits of experimental error.

Three conversion vs. time curves are presented in Figures 6, 7, and 8. Figure 6 represents the conversion time behavior for a single kettle run and indicates the absence of scatter in conversion data taken from a single reaction vessel for a run in progress. Figure 7 is a composite rate curve combining rate data from two kettle runs with data from several bottle reactors. In the case of the bottle reactor only one data point is taken from each bottle. Thus, the scatter in Figure 7 represents the difficulty in exactly duplicating conditions between reactors rather than any difficulty in accurately obtaining conversion data on a sample taken from a reactor or a single bottle. The problem of reproducing conditions between reactors is discussed in greater detail in Appendix A. Figure 7 is presented to show an average conversion-time behavior for the standard formulation of this study. It should be particularly noticed that constant rate behavior is exhibited between 0 and 60 percent conversion. From 60 to 90 percent conversion the conversion rate increases and then tapers off until polymerization is completed. The

average conversion rate during the constant rate period is 13%/hr. ± 2%/hr.

Figure 8 represents a kettle run that was perturbed after 80 minutes by the addition of 0.5 gms. of additional $K_2S_2O_8$. As shown, the addition of initiator during the constant rate period does not alter the shape of the curve up to about 60 percent conversion even though the rise in rate after 60 percent conversion (associated with the Trommsdorff effect) is more pronounced. In accordance with previous discussion this indicates that behavior during the constant rate period is indeed ideal with $\bar{n} = \frac{1}{2}$. The system, therefore, has all of the characteristics of the Smith-Ewart kinetics for polydisperse formulations.

FIGURE 6

CONVERSION vs. TIME FOR A SINGLE KETTLE RUN KI

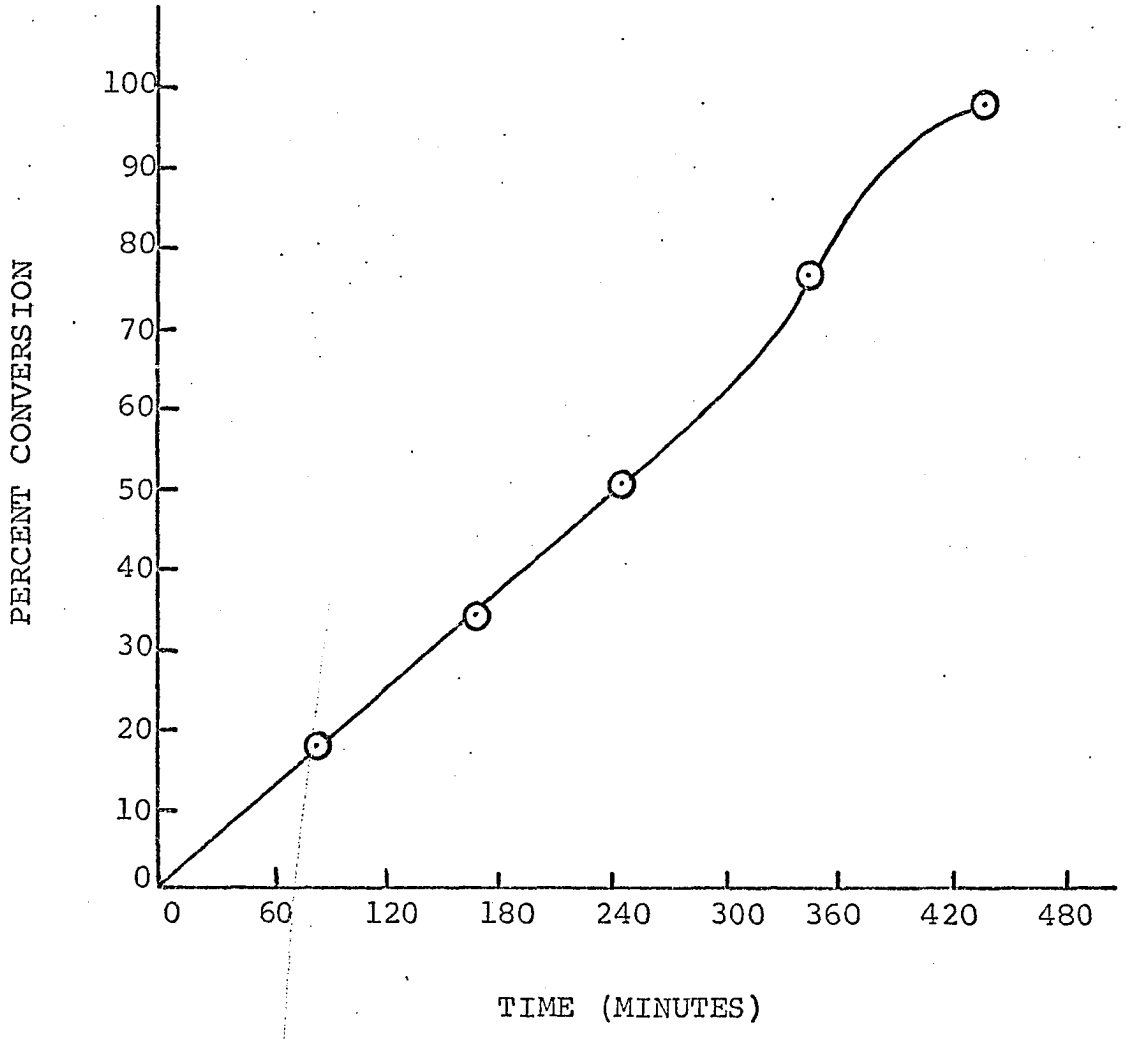

FIGURE 7

PERCENT CONVERSION vs. TIME

COMPOSITE CURVE

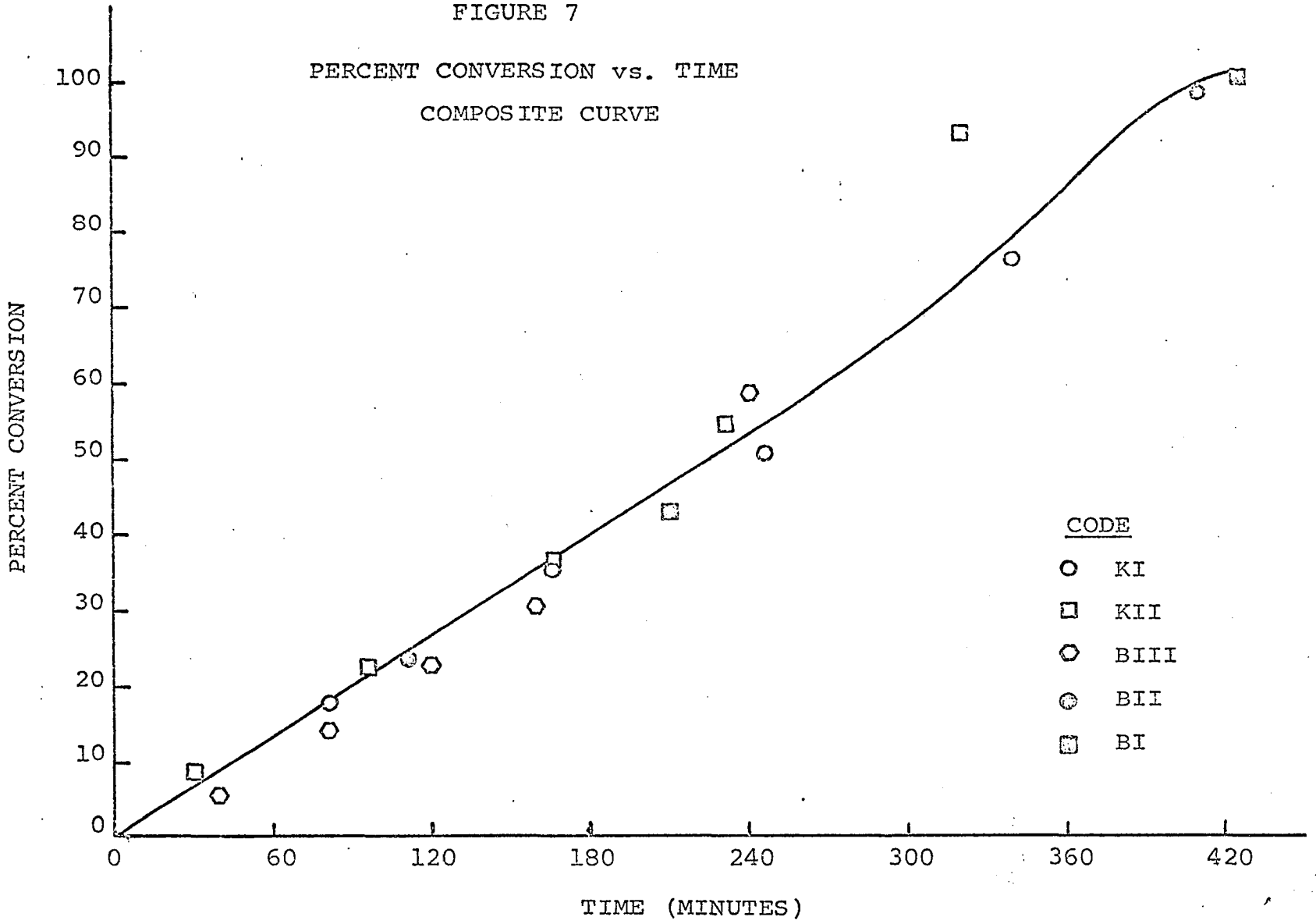

FIGURE 8

CONVERSION vs. TIME

INITIATOR - ADDITION

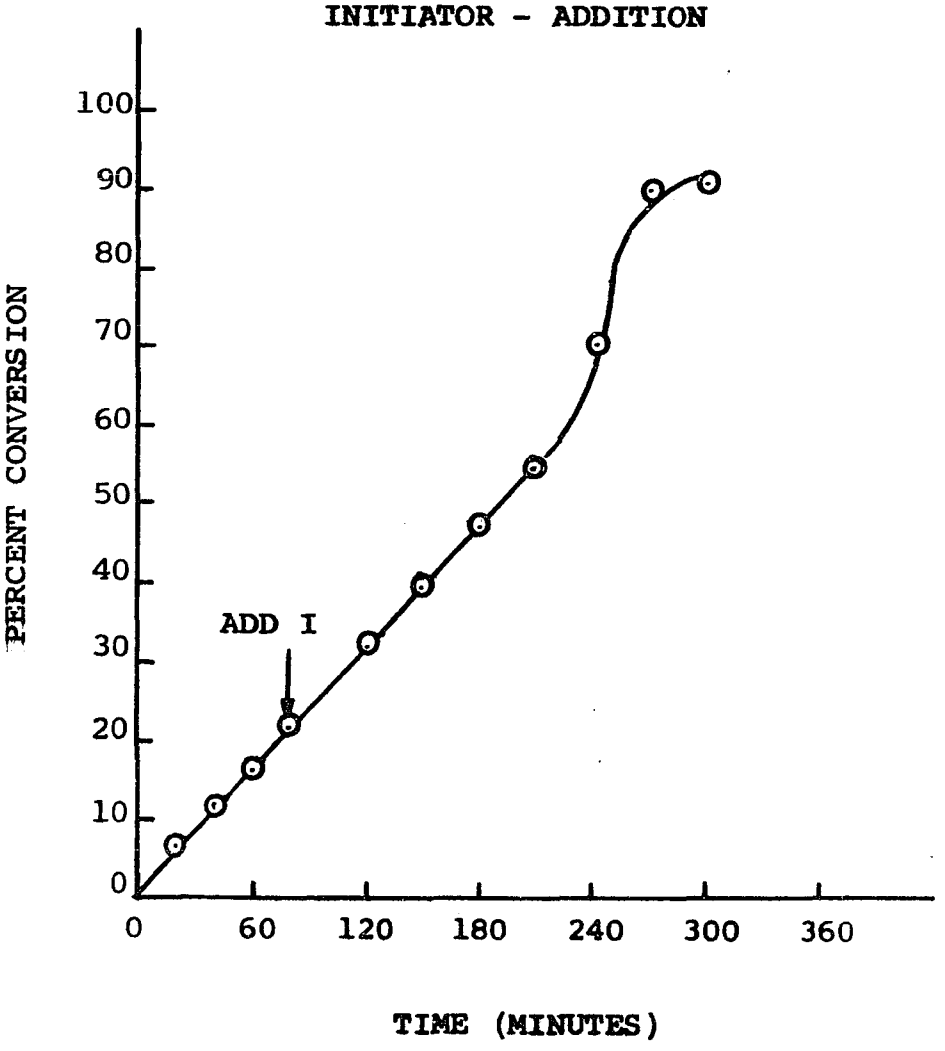

E - Molecular Weight Development

1 - Introduction

The discussion of molecular weight development has been divided into two major sections. In the first section, final results and conclusions are discussed, molecular weight trends are analyzed, and the problem of molecular weight increase during ideal emulsion polymerization is defined by comparison of measured and predicted molecular weights. Experimental data points, techniques, and the discussion of error have been omitted from this section.

The second section deals with the raw data used to obtain the smoothed curves discussed in the first section. Detailed experimental data are presented and it is shown that experimental error is at least an order of magnitude smaller than the trends being discussed. The discussion has been arranged in this order for clarity and continuity in the discussion of results. A third section is concerned with molecular weight distribution.

2 - Discussion of Results

Results of the experimental investigation of molecular weight development are summarized in Figure 9. Previously published molecular weight development data for styrene emulsion polymerization deal with viscosity average molecular weight. Thus, viscosity average molecular weight is followed to provide a basis of comparison between the present study and the literature. In order to make a valid comparison with theory, however, number average molecular weight must also be considered. The viscosity average molecular weight is sensitive to branching and transfer while the number average is not. This dissertation presents the first published report of number average molecular weight development during ideal styrene emulsion polymerization.

Actual molecular weight measurements, naturally, yield a cumulative average. It is more useful, however, to follow the instantaneous molecular weight*, or kinetic chain length, development as an index of changing conditions. Instantaneous molecular weights were simply determined from material balances on the cumulative molecular weight curves. (Appendix D).

*Instantaneous molecular weight is defined as the molecular weight of the polymer being generated at any instant of time.

The predicted instantaneous number average molecular weight curve is calculated from steady state theory by means of:

$$(12) \quad \bar{x}_n = \frac{R_{pp}}{k_D[I_o]} e^{k_D t}$$

with an experimentally determined decomposition constant, k_D. The experimental determination of k_D, and the details of the calculation are discussed at length in the next section. The predicted curve represents molecular weight development that is consistent with the initiator kinetics of the system being studied if current steady state theory as expressed in equation (12) is accurate.

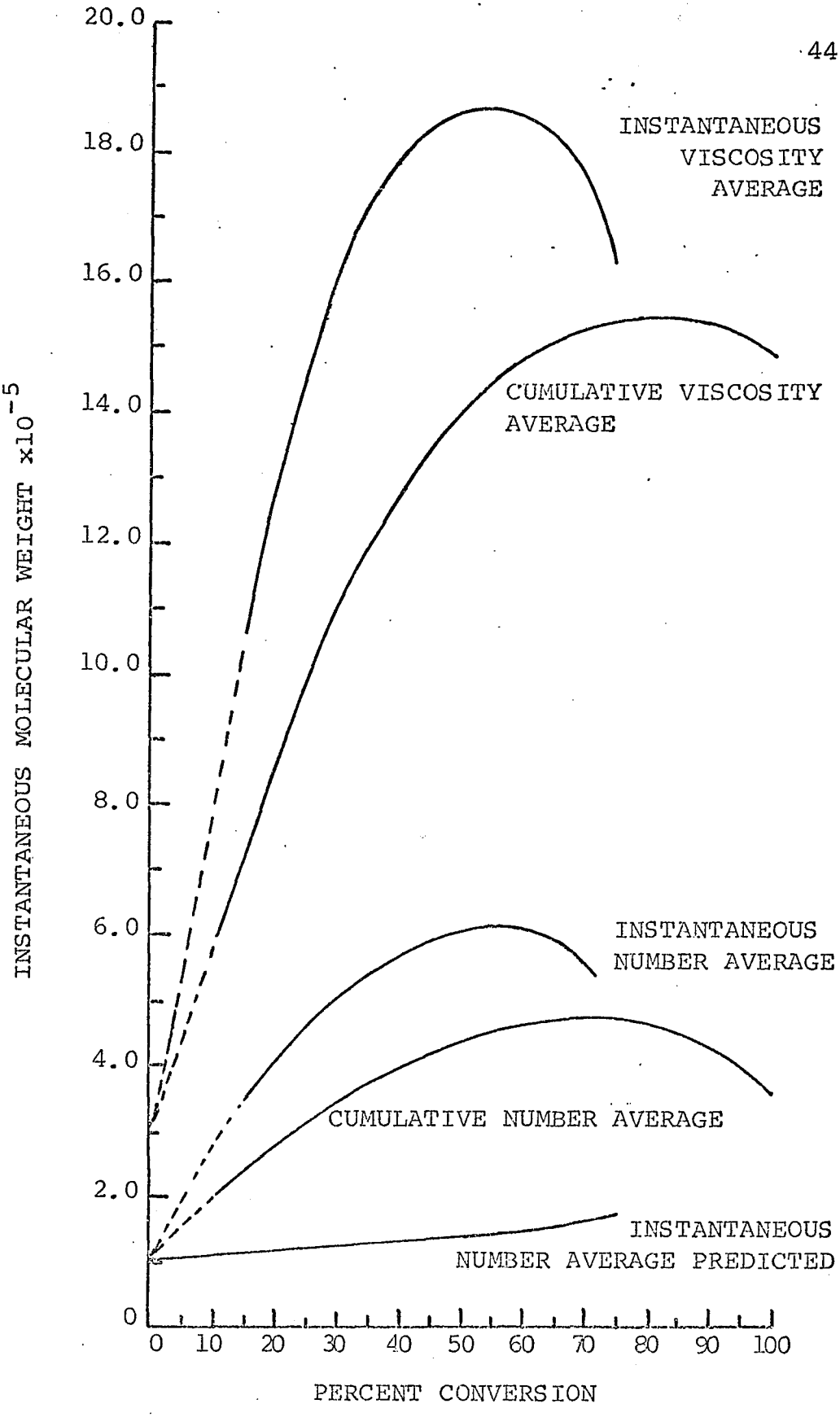

FIGURE 9: MOLECULAR WEIGHT vs. CONVERSION. CUMULATIVE, INSTANTANEOUS AND PREDICTED AVERAGE VALUES.

Consider the conclusions to be drawn from Figure 9:

1 - The molecular weight curves are typical and "ordinary." The cumulative viscosity average molecular weight development curve is similar to those reported by Williams and Bobalek (11) and Smith (5) for similar type systems. Further, the cumulative number average curve is similar in shape to the cumulative viscosity average curve. The ratios of cumulative viscosity to number average and instantaneous viscosity to number average molecular weight are compiled in Table 2. It can be seen that in both cases the viscosity to number average molecular weight ratio does not change drastically during polymerization. (The slight increase in the cumulative ratio is expected because of the continuous increase in molecular weight during the reaction.) This is indicative of a "normal" mode of polymerization.

2 - Molecular weight increase during the ideal period, between 0 and 60% conversion, is definite and significantly large. The cumulative viscosity average molecular weight increases about 500% from 300,000 to 1,500,000 while the instantaneous viscosity average molecular weight increases 600% from 300,000 to 1,900,000 during the ideal period. During this same period the cumulative number average molecular weight increases 450% from 110,000 to 480,000 while the instantaneous number average molecular weight increases 600% from 110,000 to 630,000.

TABLE 2

TABULATION OF DATA FROM AVERAGE MOLECULAR WEIGHT CURVES

FIGURE 9

%C	$\bar{M}_{v\ cum} \times 10^{-6}$	$\bar{M}_{vi} \times 10^{-6}$	$\bar{M}_{n\ cum} \times 10^{-6}$	$\bar{M}_{ni} \times 10^{-6}$	$\left(\frac{\bar{M}_v}{\bar{M}_n}\right)_{cum}$	$\left(\frac{\bar{M}_v}{\bar{M}_n}\right)_i$
10	0.60		0.200		3.00	
15		1.06		0.350		3.04
20	0.85		0.275		3.09	
25		1.44		0.452		3.18
30	1.08		0.345		3.14	
35		1.71		0.543		3.14
40	1.27		0.395		3.21	
45		1.84		0.595		3.10
50	1.40		0.430		3.26	
55		1.88		0.620		3.04
60	1.49		0.455		3.28	
65		1.81		0.592		3.06
70	1.54		0.475		3.26	
75		1.62		0.455		5.23
80	1.55					

$(\bar{M}_v)_{cum}$ = Cumulative viscosity average molecular weight

$(\bar{M}_v)_i$ = Instantaneous viscosity average molecular weight

$(\bar{M}_n)_{cum}$ = Cumulative number average molecular weight

$(\bar{M}_n)_i$ = Instantaneous number average molecular weight

3 - The molecular weight development curves show three distinct regions of behavior. Consider the instantaneous number average molecular weight curve as a specific example. From 0 to 26 percent conversion the molecular weight increases steeply from 110,000 to 460,000 or about 4.5 times. From 26% to 60% conversion the molecular weight increases less rapidly from 460,000 to 630,000 or only 0.5 times. Thus there appear to be two regions of molecular weight development during the ideal period. Beyond 60% conversion the instantaneous number average molecular weight begins to decrease. The significance of this three region behavior will be underscored in later sections.

4 - There is a definite conflict between current steady state theory and observation. If the measured instantaneous number average molecular weight is extrapolated to zero time the molecular weight determined is in complete agreement with that predicted from steady state theory and the decomposition data. As the reaction proceeds, however, the measured instantaneous molecular weight rapidly deviates from that predicted. As Figure 9 shows, the shapes of the experimental and predicted curves are at variance. The measured curve rises steeply, tapers off, and eventually begins to decrease, whereas the predicted curve is a sluggishly increasing exponential. Table 3 further indicates that the ratio of predicted to measured molecular weight starts off at about 1.0,

drops to about 0.250 by 30% conversion and changes slightly between 30 and 60% conversion. After 60% conversion the ratio begins to rise. This, again, is indicative of the three region behavior noticed earlier.

The close agreement between measured and predicted molecular weights at zero time is indicative of the internal consistency of the molecular weight and decomposition data. The discrepancy between measured and predicted molecular weights at later times indicates a phenomena which is decreasing the free radical efficiency. The numerics of Table 3 and the variant shapes of the predicted and measured molecular weight curves describe the conflict between theory and observation.

The scope of the problem can thus be stated as follows: Molecular weight increases several fold during the ideal period, and the increase cannot be explained by current steady state theory or aqueous phenomena associated with the initiator.

TABLE 3

MEASURED AND PREDICTED INSTANTANEOUS
NUMBER AVERAGE MOLECULAR WEIGHT

Percent Conversion	Instantaneous Number Average Molecular Weight Measured, $(\bar{M}_{ni})_M$	Instantaneous Number Average Molecular Weight Predicted $(\bar{M}_{ni})_p$	$\frac{(\bar{M}_{ni})_p}{(M_{ni})_M}$
0	110,000	105,000	0.960
10	280,000	110,000	0.394
20	400,000	120,000	0.300
30	500,000	125,000	0.250
40	570,000	133,000	0.233
50	610,000	140,000	0.238
60	610,000	150,000	0.246
70	550,000	165,000	0.300

3 - Discussion of the Data

a) Viscosity Average Molecular Weight

Intrinsic viscosities were determined by the one point method of Maron (36) from relative viscosities of dilute toluene solutions measured at 30°C in Cannon-Ubhelode dilution viscometers. In the exponential relationship $(\eta) = KM_v^a$ the constants of Goldberg et al. (37) were used. $K = 3.7 \times 10^{-4}$ and $a = 0.62$. $\bar{M}_v$ is the viscosity average molecular weight and (η) is the intrinsic viscosity of the dilute polystyrene-toluene solution.

The molecular weight data are compiled in Table 4. Intrinsic viscosity-conversion behavior is presented in Figure 10 and cumulative and instantaneous viscosity average molecular weight is presented in Figure 11. First, consider the viscosity average data asterisked in Table 4. Here two separate independent determinations were made on the same sample to check reproducibility. In all cases reproducibility between determinations is well within $\pm$ 5%. The asterisked data also indicate that the error in viscosity measurement is somewhat magnified in the calculation of molecular weight. Comparison of Figures 10 and 11 will further bear this out. The standard deviation within a determination is less than $\pm$ 3%.

Viscosity average samples were obtained from several different reactors as shown in Figure 11. With the exception of the 50 percent conversion sample

TABLE 4

MOLECULAR WEIGHT DATA

RUN AND SAMPLE #	%C	INTRINSIC VISCOSITY	$\bar{M}_v \times 10^{-6}$	$\bar{M}_n \times 10^{-5}$
KI - 1	17.5	1.97	0.822	2.33
2	34.1	2.51,2.52*	1.12,1.16*	3.18,3.03*
3	50.0	1.96,1.97*	0.776,0.778*	3.79
4	76.0	2.68	1.10	4.46
5	97.0	2.75,2.80*	1.25,1.36*	3.79
KII- 1	8.0	- - -	- - -	2.08
2	22.0	2.03,1.95*	0.852,0.784*	3.20
3	36.0	2.54	1.20	4.04,4.04*
4	54.0	2.83	1.30	4.88
5	92.0	3.27	1.60	4.04
BI - 6	42.0	2.89	1.44	
10	100.0	3.49	1.84	
BII- 3	23.0	2.35	1.07	
BIII-1	5.0	1.70	0.632	
2	14.0	1.75	0.735	
3	22.0	2.15	0.920	
4	30.0	2.00	0.880	
6	58.0	2.96	1.448	

*Two separate determinations to check reproducibility

KI, KII are kettle runs.

BI, BII, BIII are bottle polymerizer runs.

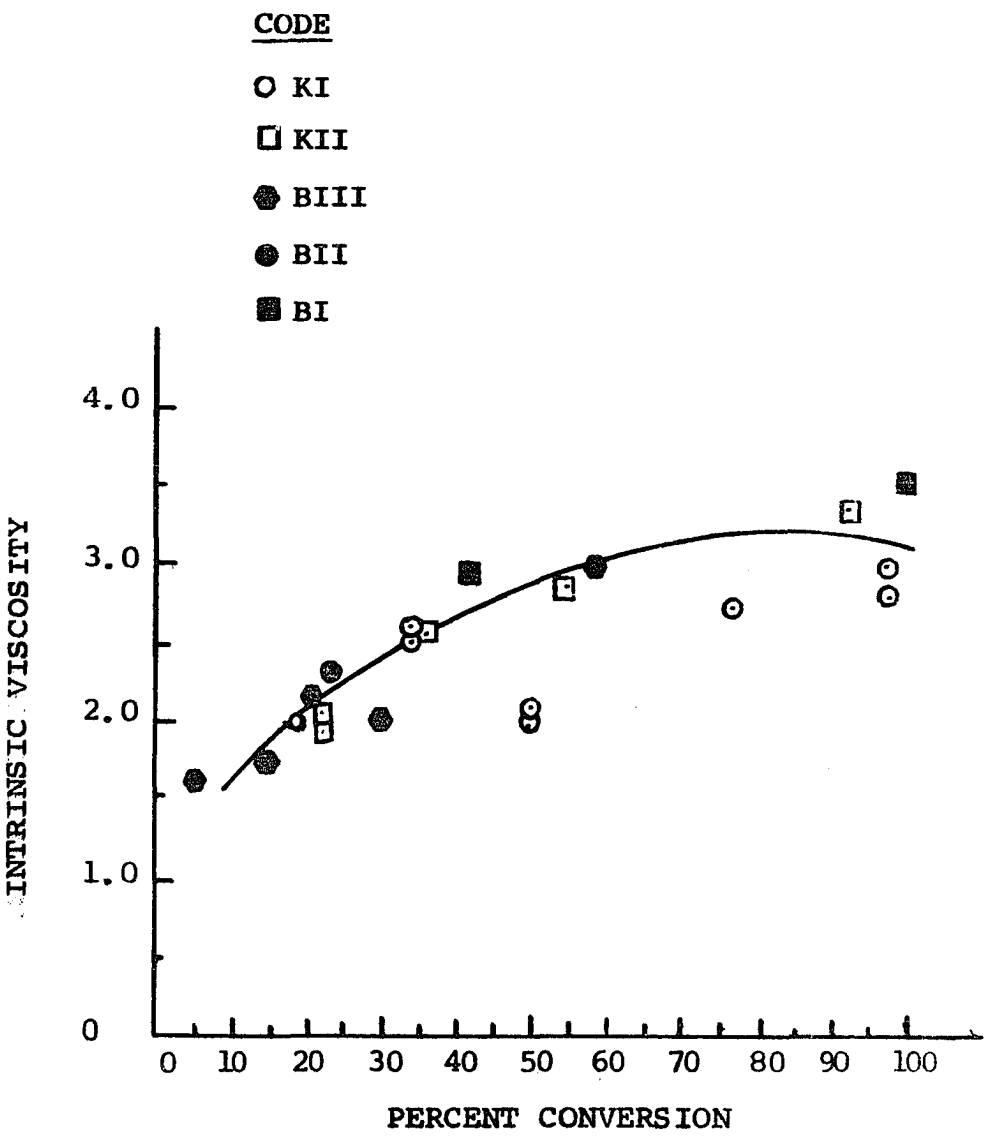

FIGURE 10: INTRINSIC VISCOSITY vs. CONVERSION

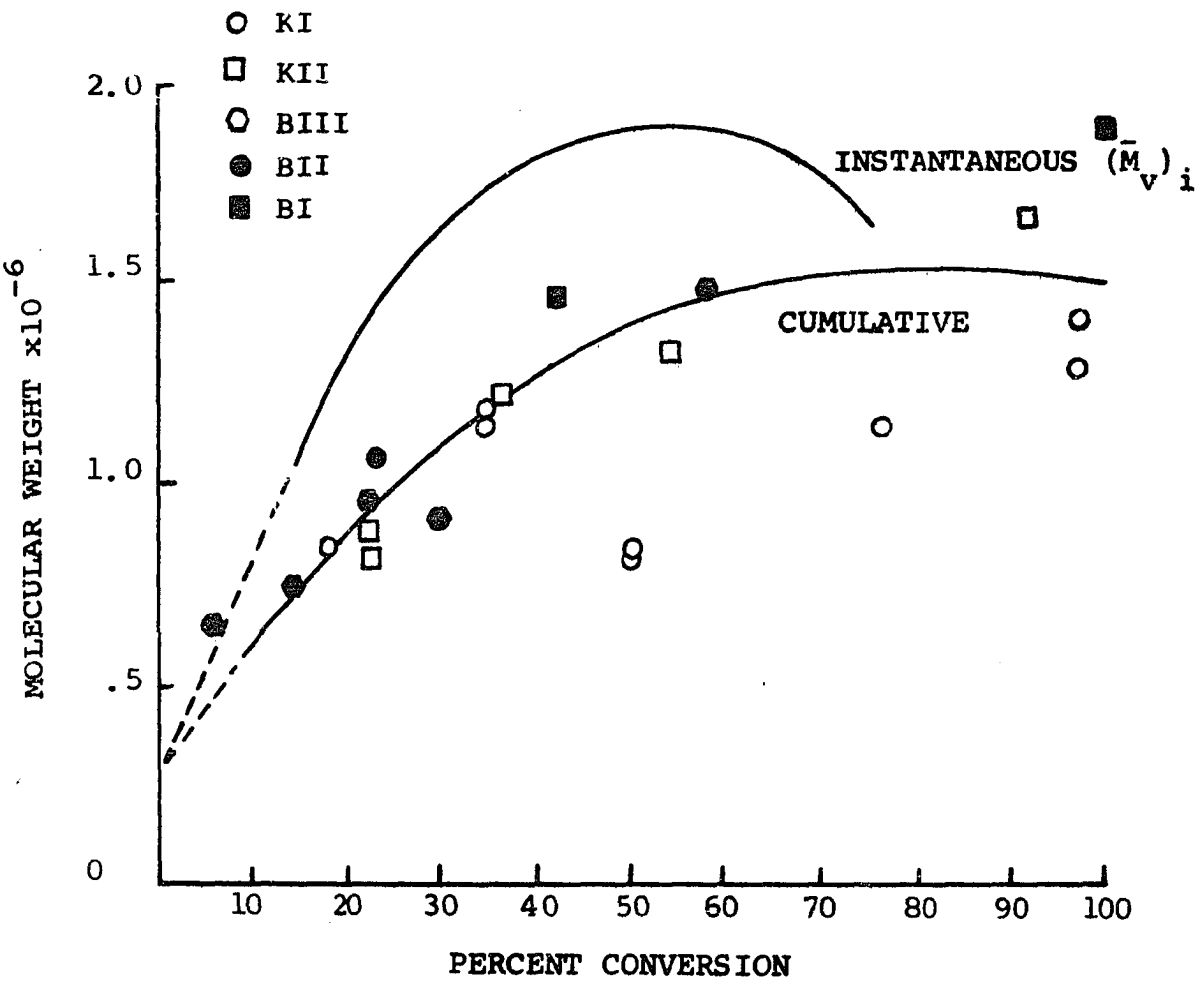

FIGURE 11 - VISCOSITY AVERAGE MOLECULAR WEIGHT CUMULATIVE AND INSTANTANEOUS ($\bar{M}_{vi}$)

from run KII, all of the cumulative molecular weight data points between 0 and 60% conversion lie within ± 15% of the average curve; in fact, half of the data points in this range are on the average curve. If one were to consider any one reactor the scatter in the data would be even less. Much of the scatter can be ascribed to the difficulty in exactly reproducing conditions within a reactor between runs. The instantaneous viscosity average molecular weight curve was drawn from the average cumulative curve.

In the previous section molecular weight increases on the order of hundreds of percent were considered. Here, it has been shown that the maximum scatter in the data is ± 15%. The scatter, then, is an order of magnitude smaller than the trends being considered.

b) Number Average Molecular Weight

Number average molecular weights were determined from osmotic pressure via the limiting law of van't Hoff. Osmotic pressures were measured with a Mechrolab 501 high speed osmometer utilizing an Arro 300-D gel cellophane membrane. Toluene solutions were used at 37°C.

The molecular weight data are compiled in Table 4 where the asterisked data again indicate that number average molecular weight measurements for

a given sample were reproducible to within ± 5%. Measurements within a given determination were likewise reproducible to within ± 5% (Appendix D).

Number average molecular weight samples were taken from kettle runs KI and KII. The cumulative average data points for the two runs lie on smooth curves which are essentially parallel as shown in Figure 12. In Figure 12, an average molecular weight curve is drawn between the curves for runs KI and KII. Run KII was characterized by a conversion rate of 15 percent per hour and run KI by a rate of 12 percent per hour. Since the average conversion rate for the system studied was 13 ± 2% per hour, the average curve should, indeed, be descriptive of the system. Either molecular weight development curve (KI or KII) lies within ± 10% of the average curve. Instantaneous number average molecular weights were calculated from runs KI and KII separately and listed in Table 5. The results are presented graphically in Figure 13 where it is again seen that each curve lies within ± 10% of an average curve. The predicted instantaneous number average molecular weight is also presented in Figure 13, but discussion of this curve will be reserved until later.

The smooth behavior of the individual molecular weight curves for runs KI, KII underscores the fact that scatter in the data is basically a result

of difficulty in exactly reproducing conditions between runs based on the same formulation. It should be noted here that the problem of reproducibility is characteristic of emulsion polymerization studies in general and therefore not unique to this study. Further, the scatter or spread of $\pm$ 10% in the data is, again, an order of magnitude less than the molecular weight increase discussed in the preceding section.

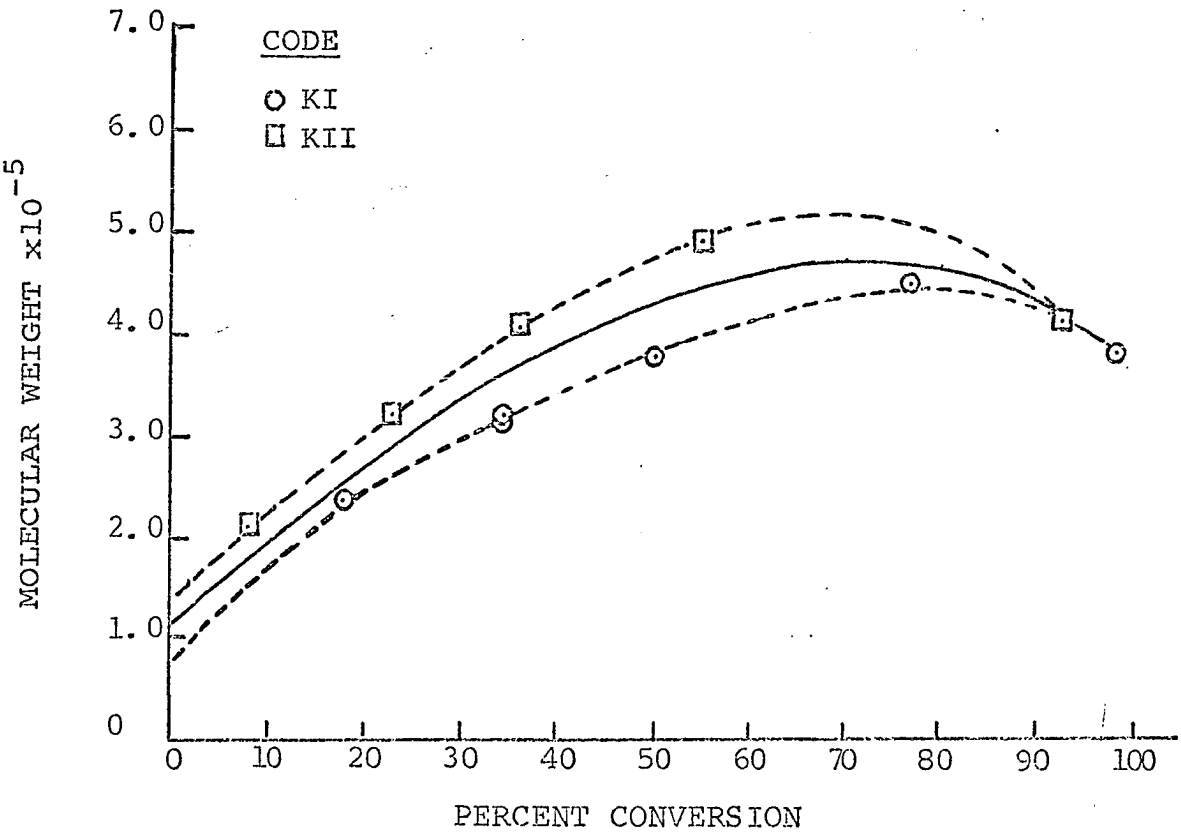

FIGURE 12 - NUMBER AVERAGE MOLECULAR WEIGHT, CUMULATIVE

TABLE 5

INSTANTANEOUS NUMBER AVERAGE MOLECULAR WEIGHTS CALCULATED FOR RUNS KI, KII

	RUN KI		RUN KII	
%C	CUMULATIVE NUMBER AVERAGE $(\bar{M}_n)_{CUM.}$	INSTANTANEOUS NUMBER AVERAGE $(\bar{M}_n)_i$	CUMULATIVE NUMBER AVERAGE $(\bar{M}_n)_{CUM.}$	INSTANTANEOUS NUMBER AVERAGE $(\bar{M}_n)_i$
10	1.65×10^5		2.25×10^5	
15		3.05×10^5		3.95×10^5
20	2.35×10^5		3.10×10^5	
25		4.00×10^5		5.05×10^5
30	2.90×10^5		3.75×10^5	
35		4.90×10^5		5.75×10^5
40	3.40×10^5		4.25×10^5	
45		5.40×10^5		6.50×10^5
50	3.80×10^5		4.70×10^5	
55		5.90×10^5		6.50×10^5
60	4.15×10^5		5.00×10^5	
65		5.80×10^5		6.05×10^5
70	4.40×10^5		5.15×10^5	
75		5.20×10^5		3.95×10^5
80	4.50×10^5		5.00×10^5	

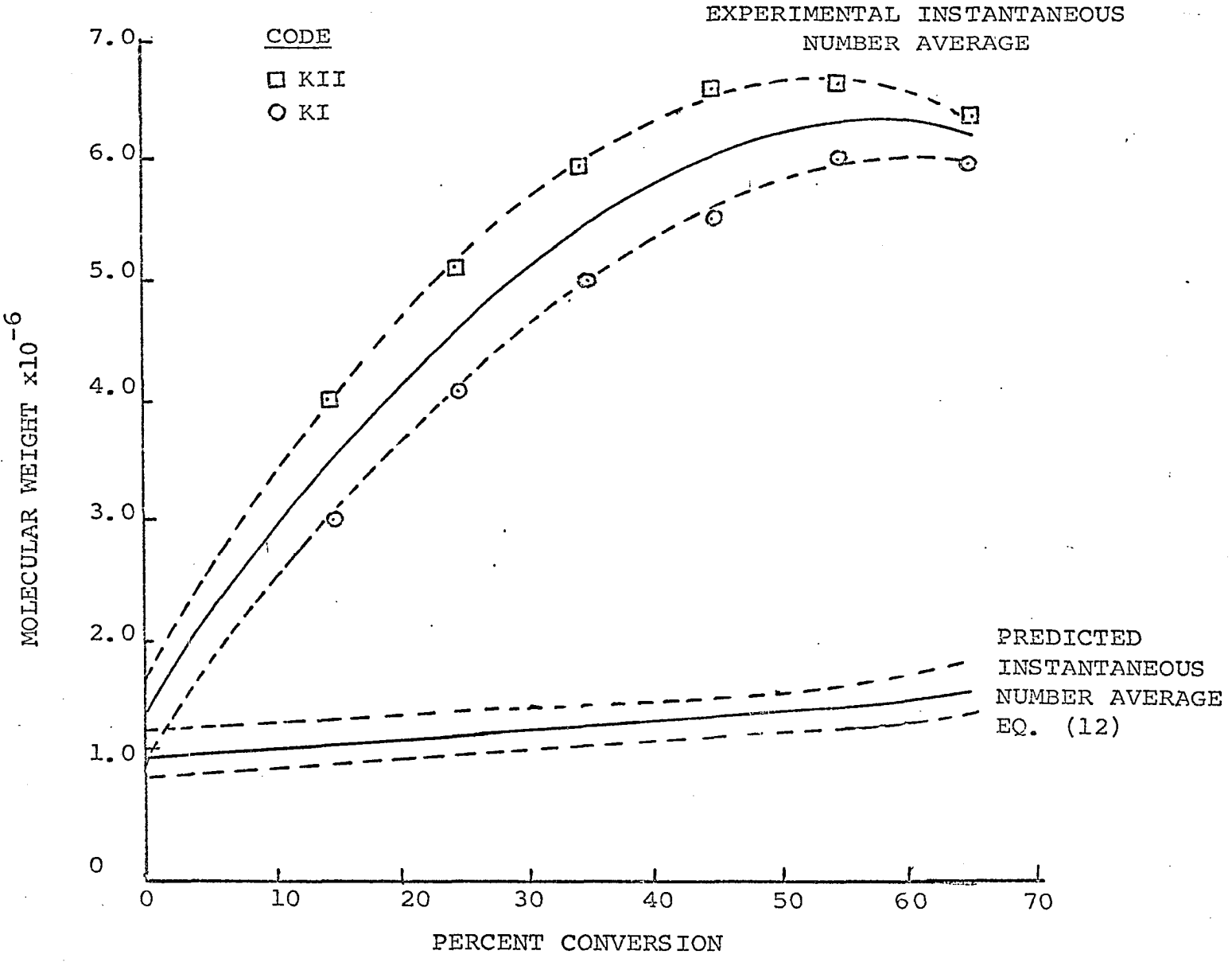

FIGURE 13 - INSTANTANEOUS NUMBER AVERAGE MOLECULAR WEIGHT

c - Initiator Kinetics

As mentioned earlier, a thorough understanding of molecular weight development hinges upon a knowledge of initiator kinetics. This involves knowledge of the rate of initiator decomposition and the rate of free radical generation. For a system in which side reactions do not occur these two rates should be equal. A general discussion of initiator kinetics follows.

1 - Initiator Decomposition

The rate of persulfate decomposition in alkaline soap solution was determined via an iodine titration technique initially developed by Kolthoff et al. (28, 38). Attempts at direct titration of a latex failed because of end point obscurity so the titrations were carried out in a simulated environment in the absence of latex or monomer. Solutions containing 180 g. water, 3.00 g. Triton X-100, 0.15 g. sodium lauryl sulfate, 0.075 g. KOH, and 0.500 g. $K_2S_2O_8$ were charged in bottles. The bottles were then placed in the bottle polymerizer for from one to four hours at 60 $\pm$ 1°C, withdrawn, and cooled in ice water. Two kettle runs were also made at 3 hours and 4-3/4 hours. The reactor samples were acidified with acetic acid. Ten grams of KI were added and allowed to react with the residual $K_2S_2O_8$ for 30 minutes with agitation. The released iodine was titrated quantitatively with sodium thiosulfate.

The scatter in the data was attributed primarily to two phenomena. First, the soap solution foamed making titration difficult. Secondly, the presence of surfactant masked the effect of the starch indicator. Although the data will not be presented until Appendix E, it was definitely established that the presence of KOH and surfactant did not affect the validity of the titration. Further, it was established that the presence of soap and KOH significantly affected the decomposition kinetics. The $K_2S_2O_8$ was found to decompose four times faster in the alkaline soap solution.

Table 6 and Figure 14 indicate that the decomposition of potassium persulfate in aqueous alkaline (pH=9) soap solution is first order with $k_D = 1.30 \times 10^{-3} min^{-1}$. This value is more than three times greater than that determined by Kolthoff et al. (28) in the absence of soaps. In Figure 14, the two dotted lines represent bounds on the data. The high bound indicates $k_D = 1.55 \times 10^{-3} min^{-1}$ while the low bound yields $k_D = 1.05 \times 10^{-3} min^{-1}$. Thus the maximum error in using $k_D = 1.3 \times 10^{-3} min^{-1}$ is $\pm$ 20%. These data and their implication in molecular weight development will be discussed after a consideration of free radical generation rates.

TABLE 6

% DECOMPOSITION OF $K_2S_2O_8$ IN ALKALINE SOAP SOLUTION

Reaction Time:	1 hr.	2 hr.	3hr.	4 hr.	4 hr. 45 min.
	8.2%	16.4%	22.7%*	26.6	27.7*
	5.6%	9.3%	20.6%	24.0	---
	10.1%	10.0%	22.9%	25.8	---
	---	---	25.3%	23.3	---

*Kettle Runs

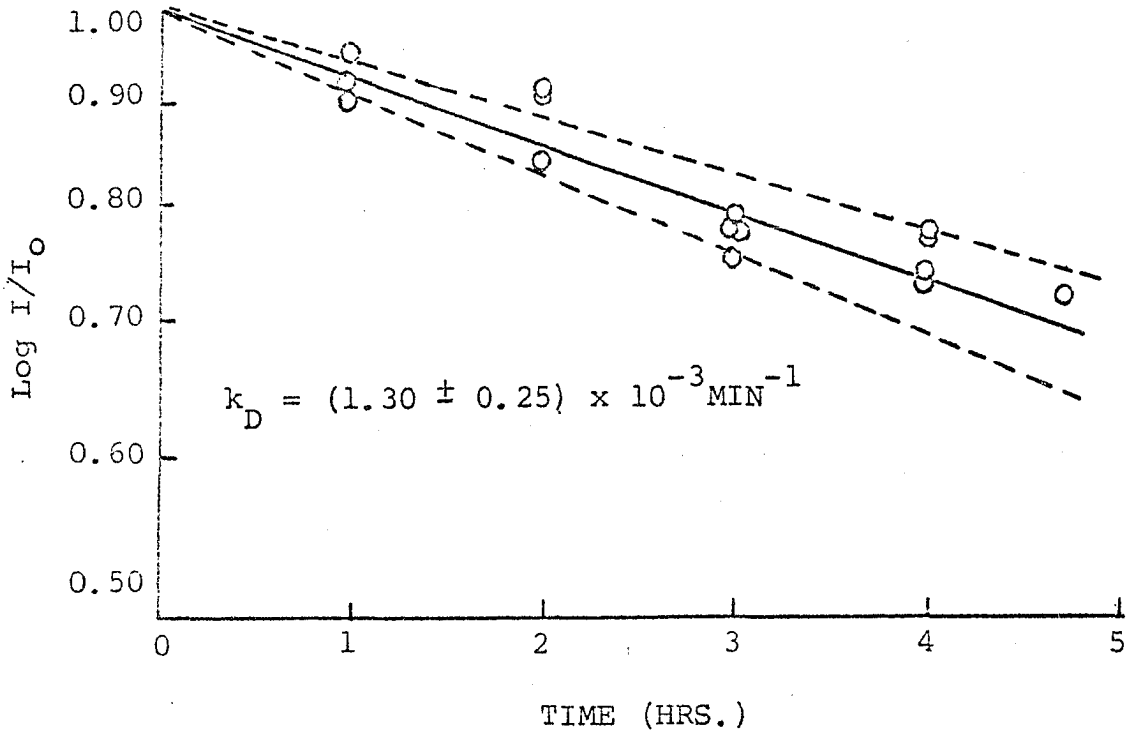

FIGURE 14 - DECOMPOSITION OF $K_2S_2O_8$ IN ALKALINE SOAP SOLUTION

2 - Free Radical Generation

In situ inhibitor studies were conducted to measure free radical generation rates in the actual aqueous reaction medium. This was done to verify and amplify the decomposition data. Here an aqueous solution of paraquinone was added to a reaction, one, two, or three hours in progress and the radical generation rate was measured by the length of the induction period before reaction resumed. See Figure 15 as a sample curve.

The paraquinone-radical reaction scheme which best fits the data is one based on the work of Read and Price (39) (see Appendix E) in which two moles of quinone are consumed for each mole of radical captured, or, four moles of quinone are consumed for each mole of $K_2S_2O_8$ decomposed.

The in situ induction period studies with water soluble inhibitors verified the nature of the aqueous phase free radical generation process. Comparison of columns E and F in Table 7 show that the measured induction periods are in close agreement with those predicted from decomposition data. Thus, free radicals are formed in the aqueous phase by a 100% efficient first order decomposition of persulfate, and the presence of dissolved monomer, latex, and the physical location of the soap do not alter the decomposition kinetics derived from the aqueous soap solution studies. The agreement between the two techniques is reassuring, but the inhibitor method is probably the most

direct and useful general approach in such studies.

Furthermore, comparison of runs 1, 4, 6, and 7, from Table 7, in which 0.032 g. of paraquinone have been added to reactions 15, 60, 120, and 180 minutes in progress show that there is no unusual variation in the radical generation process throughout the course of a run. To verify the quantitative nature of the study, notice that runs 2, 3, and 4 show that the induction period is directly proportional to the quantity of inhibitor added. Further, comparison of runs 4 and 5 underscores the reproducibility of the measurements.

TABLE 7

INHIBITOR DATA

	A REACTION TIME (MIN.)	B %C/hr.	C PQ	D INDUCTION PERIOD (MIN.)	E ADJ. IND.PD.	F EXPECTED IND. PD.
1	15	12.0	0.032	32.0	29.6	29
2	60	14.5	0.008	7.0	7.8	7.5
3	60	13.4	0.016	13.0	13.5	15
4	60	10.6	0.032	36.0	29.4	30
5	60	10.3	0.032	36.0	28.6	30
6	120	12.8	0.032	32.0	31.2	33
7	180	15.4	0.032	30.0	35.5	36

A: Reaction time at which inhibitor was added. (MIN.)

B: Conversion rate before addition of inhibitor (%C/hr.)

C: Quantity of paraquinone added (gm.)

D: Measured induction period (min.)

E: Induction period adjusted to an initial conversion rate of 13.0%/hr. Obtained by multiplying the measured induction period by the ratio of Col. B to 13.0. (see Appendix E).

F: Expected induction period based on reaction mechanism, decomposition data, and 100% radical generation efficiency.

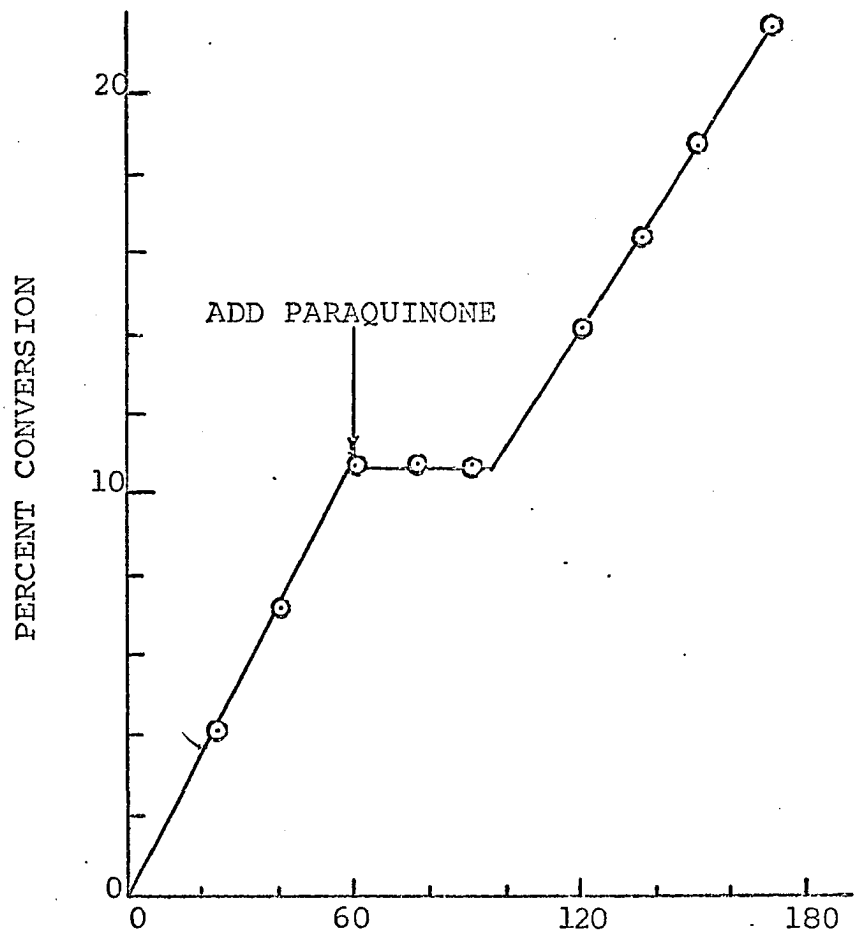

FIGURE 15 - SAMPLE INHIBITOR CURVE
(TABLE 5, RUN 4)
0.032 GM OF PARAQUINONE
ADDED TO STANDARD RUN
AFTER 60 MINUTES

3 - Predicted Instantaneous Number Average Molecular Weight

The instantaneous number average molecular weight was calculated using equation (12).

$$\bar{X}_n = \frac{R_{pp}}{k_D I_o} e^{k_D t} \qquad (12)$$

along with an average conversion rate of 13% per hour and the initiator kinetics discussed in this section. The calculation was performed with the high, low and average values of k_D and the results tabulated in Table 8.

In Figure 13 both the measured and predicted instantaneous number average molecular weights are presented with the dotted lines representing the maximum bounds of error. Visual observation of Figure 13 reveals that experimental scatter does not, in any way, cloud interpretation of trends in the data. The conflict between observation and steady state theory is, thus, clearly outlined in Figure 13.

TABLE 8

INSTANTANEOUS NUMBER AVERAGE MOLECULAR WEIGHT CALCULATED FROM DECOMPOSITION DATA

TIME (MIN.)	% CONVERSION @ 13%/hr.	$\bar{M}_{nik}$	$\bar{M}_{niL}$	$\bar{M}_{niM}$	$\bar{M}_{niH}$
0	0	452,000	128,000	105,000	88,500
60	13	460,000	136,500	113,500	97,000
120	26	469,000	145,000	122,500	106,500
180	39	476,000	154,000	132,500	117,000
240	52	485,000	164,000	143,500	128,000
300	65	495,000	176,000	155,000	141,000

$\bar{M}_{nik}$: instantaneous number average molecular weight calculated with the decomposition constant determined in pure aqueous media by Kolthoff: $k_D = 0.3 \times 10^{-4} min^{-1}$

$\bar{M}_{niL}$: instantaneous number average molecular weight calculated with the lowest experimental value of k_D = $1.07 \times 10^{-3} min^{-1}$

$\bar{M}_{niM}$: instantaneous number average molecular weight calculated with the average experimental value of k_D = $1.30 \times 10^{-4} min^{-1}$

$\bar{M}_{niH}$: instantaneous number average molecular weight calculated with the highest experimental value of k_D = $1.55 \times 10^{-3} min^{-1}$

d - Molecular Weight Distribution

Molecular weight distribution curves for individual samples at 22%, 34%, and 36% conversion respectively are presented in Figures 16-18. The data were obtained by means of gel permeation chromatography, GPC*. The data cannot be used extensively for interpretation because of inaccuracies in determining weight fractions much beyond 1,000,000. Some useful information can be gleaned from the distribution data however. First, the distributions are similar to those reported in the literature for the final emulsion polymerization products of other systems (40). Second, the molecular weight distribution curves are similar to each other thereby indicating no radical change in polymerization mechanism during the ideal period. Thirdly, the data reveal that all polymer of molecular weight less than 6,000 has been lost in the cleaning process. Finally, for the sake of compactness the entire distribution curve has not been drawn. Nonetheless, in each instance the highest molecular weight species found was between 13 and 15 million.

*The GPC was done by Professor A.E. Hamielec of MacMaster University using samples prepared for analysis in this laboratory.

FIGURE 16

MOLECULAR WEIGHT DISTRIBUTION
SAMPLE BIII-3; 22%C

$\bar{M}_n$ = 324,000

$\bar{M}_w$ = 1,290,000

$\bar{M}_v$ = 1,050,000

$\frac{\bar{M}_w}{\bar{M}_n}$ = 3.98

HIGHEST MOLECULAR WEIGHT OBSERVED

1.53×10^7

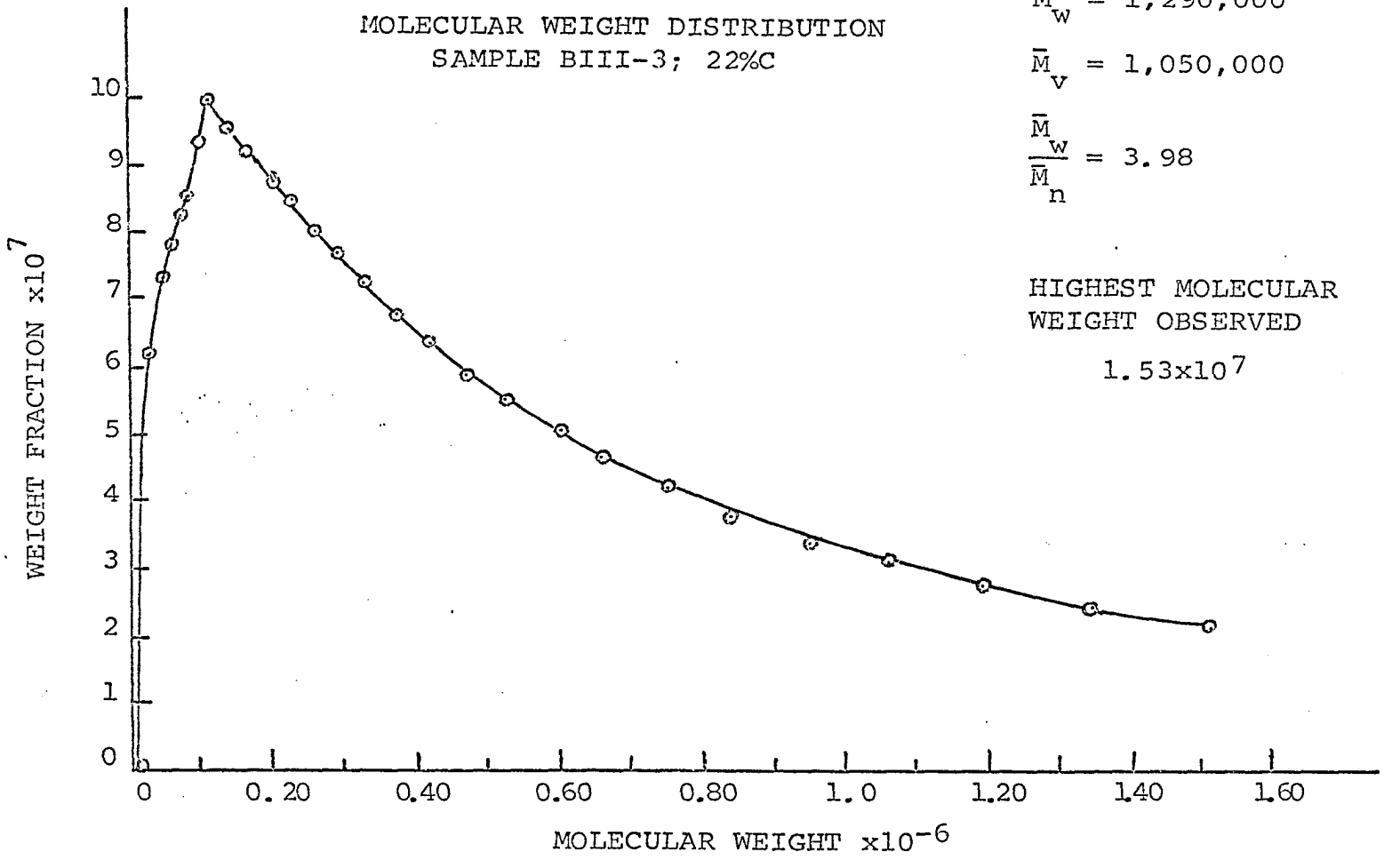

FIGURE 17

MOLECULAR WEIGHT DISTRIBUTION

SAMPLE KI-2; 34.1%C

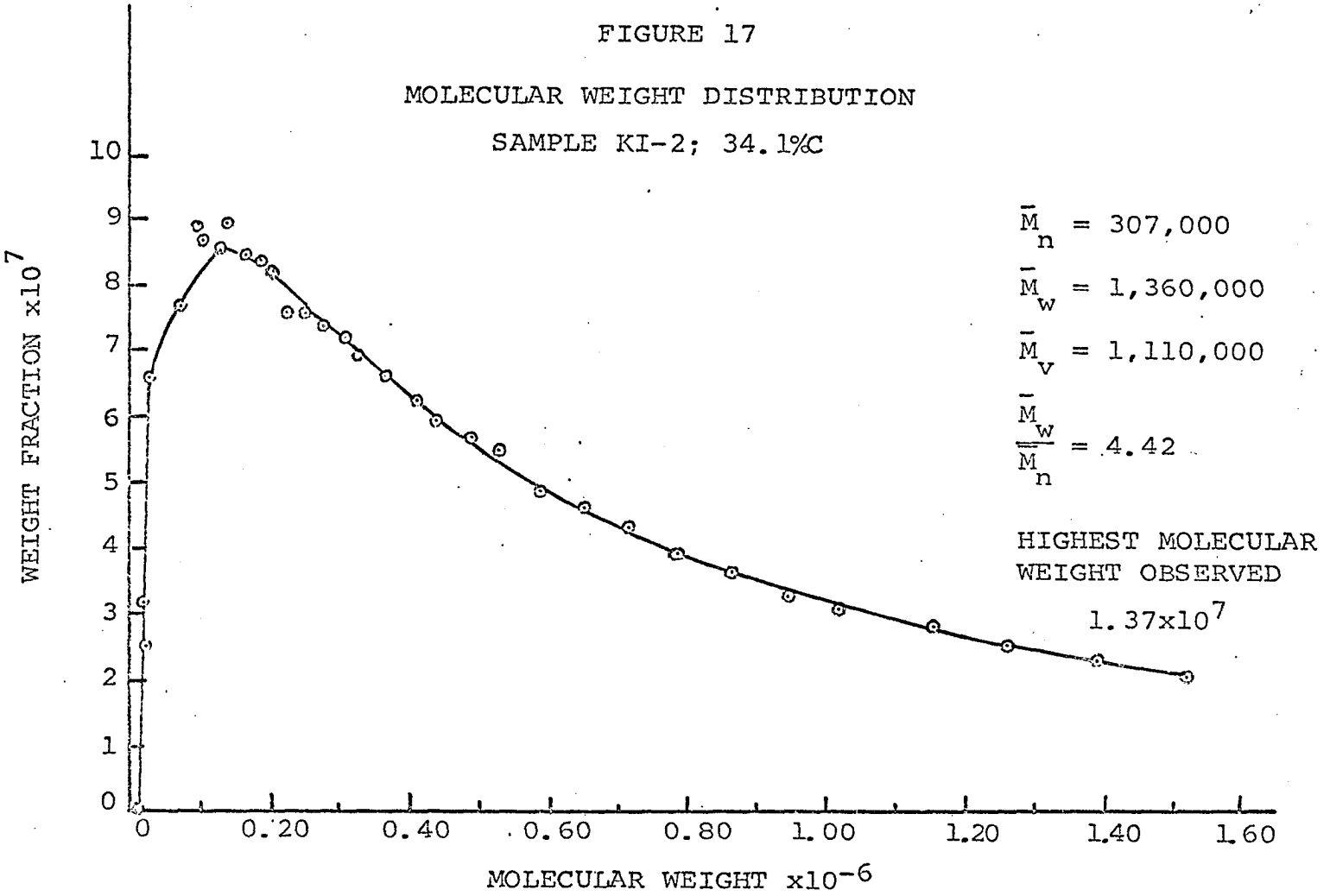

FIGURE 18

MOLECULAR WEIGHT DISTRIBUTION

SAMPLE KII-3; 36%C

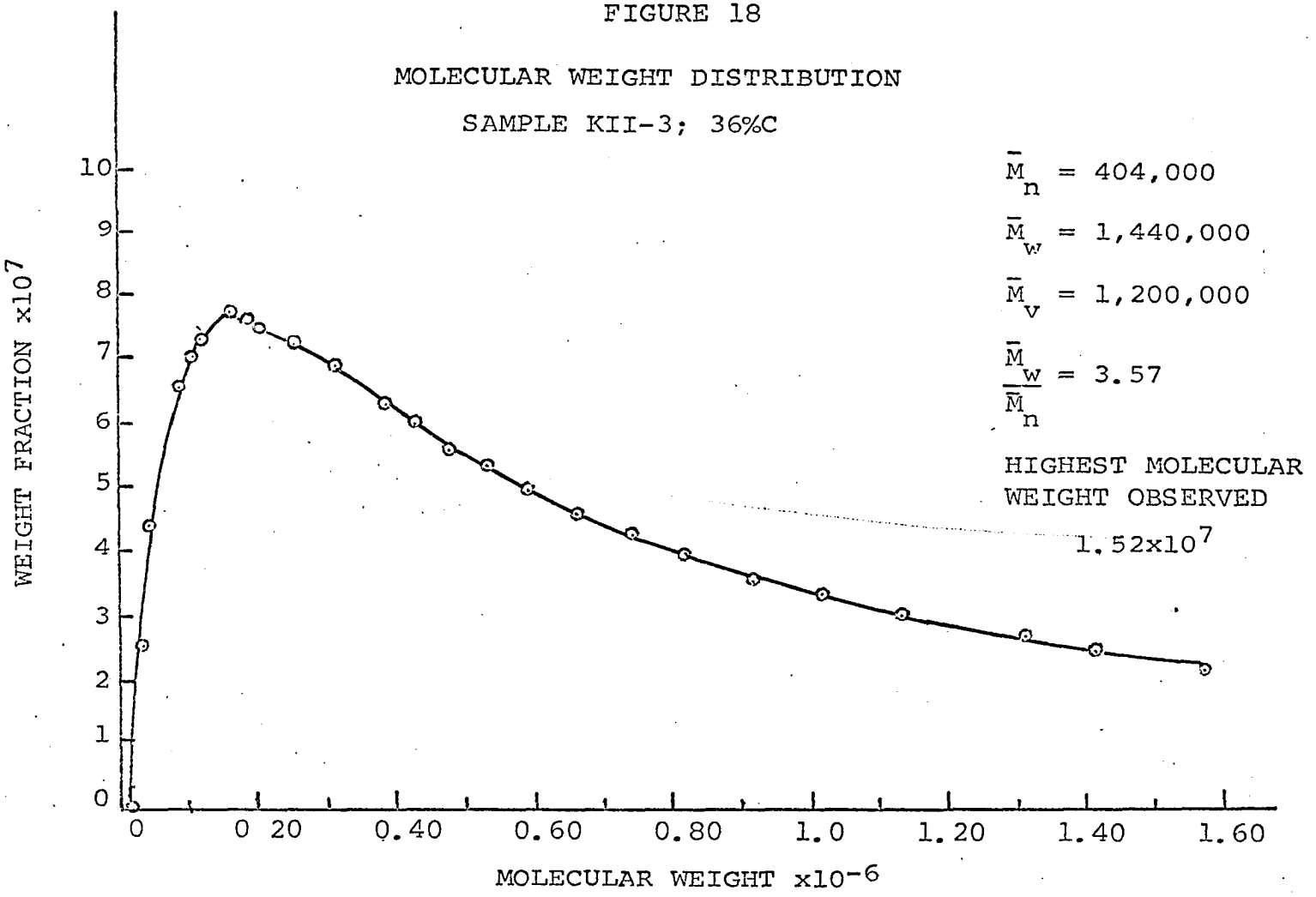

F - Monomer-Polymer Ratio

The monomer-polymer ratio was measured on unaltered samples taken from a run in progress to yield dynamic rather than equilibrium ratios. The measurement was made via gas chromatography. Samples were taken from the kettle, quenched with paraquinone, and immediately centrifuged to remove residual monomer. To insure the dynamic nature of the measurement this procedure was carried out in less than five minutes without dilution of the latex sample.

The dependence of monomer-polymer ratio on conversion for the standard formulation of this study is presented in Table 9 and Figure 19. It should be noticed that the data are taken from three separate runs with an average conversion rate of 13% per hour, and there is negligible scatter in the data.

The development of monomer-polymer ratio with conversion shows two distinct regions. First, the monomer-polymer ratio increases slightly in the range from 0 to about 26% conversion. Thereafter, the monomer-polymer ratio decreases steadily. The first period occurs in the conversion range where free monomer reservoirs are still available. Thus, as monomer is polymerized within the particle fresh monomer is continuously supplied to the particle. The slight rise in monomer-polymer ratio between 0 and 26% conversion has two possible explanations. First, it could be said that the monomer-polymer particle is never at its equilibrium monomer value and that monomer

TABLE 9

MONOMER-POLYMER RATIO AT 13%C PER HOUR

RUN & SAMPLE NUMBER	TIME (MIN.)	%C	M/P
1-1	40	9.3	2.25
2	82	18.7	2.79
3	123	28.5	2.36
4	173	39.6	1.25
2-1	20	4.2	2.50
2	60	13.4	2.69
3	100	24.7	2.77
4	140	35.3	1.45
5	180	47.6	0.835
3-1	27	4.7	2.49
2	55	9.7	2.60
3	90	17.5	2.66
4	110	21.3	2.79
5	135	27.0	2.25
6	162	32.3	1.73

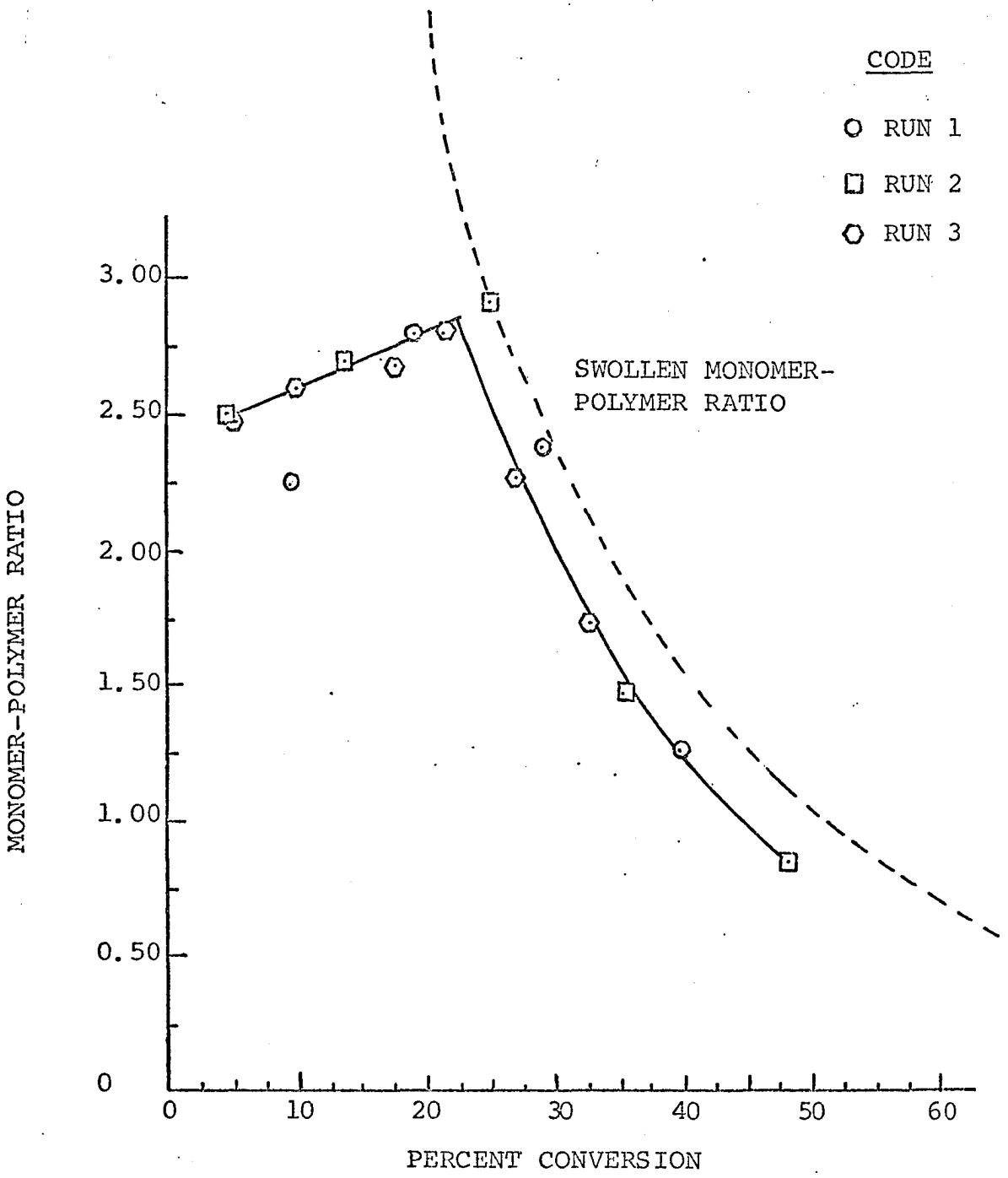

FIGURE 19 - MONOMER-POLYMER RATIO FOR STANDARD FORMULATION; CONVERSION = 13%/HR.

diffuses to the particle faster than it is being polymerized within the particle. Thus as time proceeds the monomer-polymer ratio increases as the particle tends toward an equilibrium value. A second interpretation of the data is that the monomer-polymer particle is always at equilibrium swelling, and the monomer-polymer ratio increases with increasing diameter in accordance with theory (15). In any event, there is a distinct region between 0 and 26% conversion in which the monomer-polymer ratio increases slightly.

At 26% conversion the free styrene reservoirs disappear and all of the monomer is within the monomer-polymer particle. From this point on the monomer-polymer ratio must decrease with conversion, and is fixed by the conversion. For example, at 50% conversion the monomer-polymer particle consists of 50% monomer and 50% polymer so that the monomer-polymer ratio should be 1.00. The curve calculated in this manner is shown as a dotted line in Figure 19. The measured monomer-polymer ratios in this second region lie on a curve that is almost parallel to the calculated curve but about 10% lower. Possible explanations for this deviation will be discussed in Appendix F. For now, however, it is important only to note the unmistakable general shape of the curve.

Thus, the monomer-polymer ratio first increases slightly and then decreases sharply. This is remarkable in that two region behavior with over 300% change in monomer-polymer ratio occurs during the ideal period, where the conversion rate is constant up to 60%. The data, therefore,

indicate that the rate of conversion is independent of monomer-polymer ratio. Further, it should be noted at this point that the two regions observed in monomer-polymer ratio development coincide closely with the first two regions of molecular weight development discussed earlier. Two region monomer-polymer ratio behavior shows up in these experiments because dynamic monomer-polymer ratios are measured as opposed to equilibrium swell ratios.

The bulk of this study has emphasized data accumulated for one specific formulation exhibiting 13% conversion per hour. Monomer-polymer ratios were also measured, however, for a conversion rate of 21%/hr. To accomplish this change in rate the standard formulation was simply altered by doubling the amount of sodium lauryl sulfate. The rate data are presented in Figure 20 where the constant rate period is seen to extend slightly beyond 60%C. The constant rate period is slightly longer than for the 13%/hr. run because the particle diameters for the 21%/hr. run are smaller. The slight difference between runs 4 and 5 in Table 10 is again due to the difficulty of exactly reproducing conditions between reactions utilizing the same formulation.

The monomer-polymer ratio decreases continuously as shown in Table 10 and Figure 21. The shape of the curve breaks, however, at about 35% conversion where all of the monomer is within the monomer-polymer particle. After this point the measured monomer-polymer ratio is almost coincident with the curve predicted from conversion calculations.

The data for run 5 are somewhat above the curve; this will be discussed in the Appendix. The decreasing monomer-polymer ratio in the first region is explained by reasoning that monomer is being polymerized faster than it is diffusing to the monomer-polymer particle so that the particle cannot maintain an equilibrium ratio. Again, the important point to note is that the monomer-polymer ratio is decreasing drastically and is never at equilibrium during the constant rate period. Further, the monomer-polymer ratio again shows two distinct behavioral regions.

In Figure 23 conversion and monomer-polymer ratio curves for the 13% and 21% runs are presented simultaneously, without data points. Here, it can be seen most clearly that the monomer-polymer ratio changes dramatically in both cases while the polymerization rate is constant. This data agrees in its general trends with the early work of Harkins (24).

TABLE 10

MONOMER-POLYMER RATIO AT 21%C PER HOUR

RUN AND SAMPLE NUMBER	TIME (MIN.)	%C	M/P
4-1	45	14.6	2.93
2	75	25.4	2.38
3	100	34.8	1.87
4	127	44.8	1.24
5	160	55.3	0.800
6	180	63.5	0.527
	225	84.0	
	255	88.0	
	270	90.0	
5-1	15	6.2	3.63
2	45	17.3	3.28
3	75	28.6	2.30
4	105	38.6	1.86
5	135	49.7	1.17
6	165	61.8	0.655
	225	91.0	

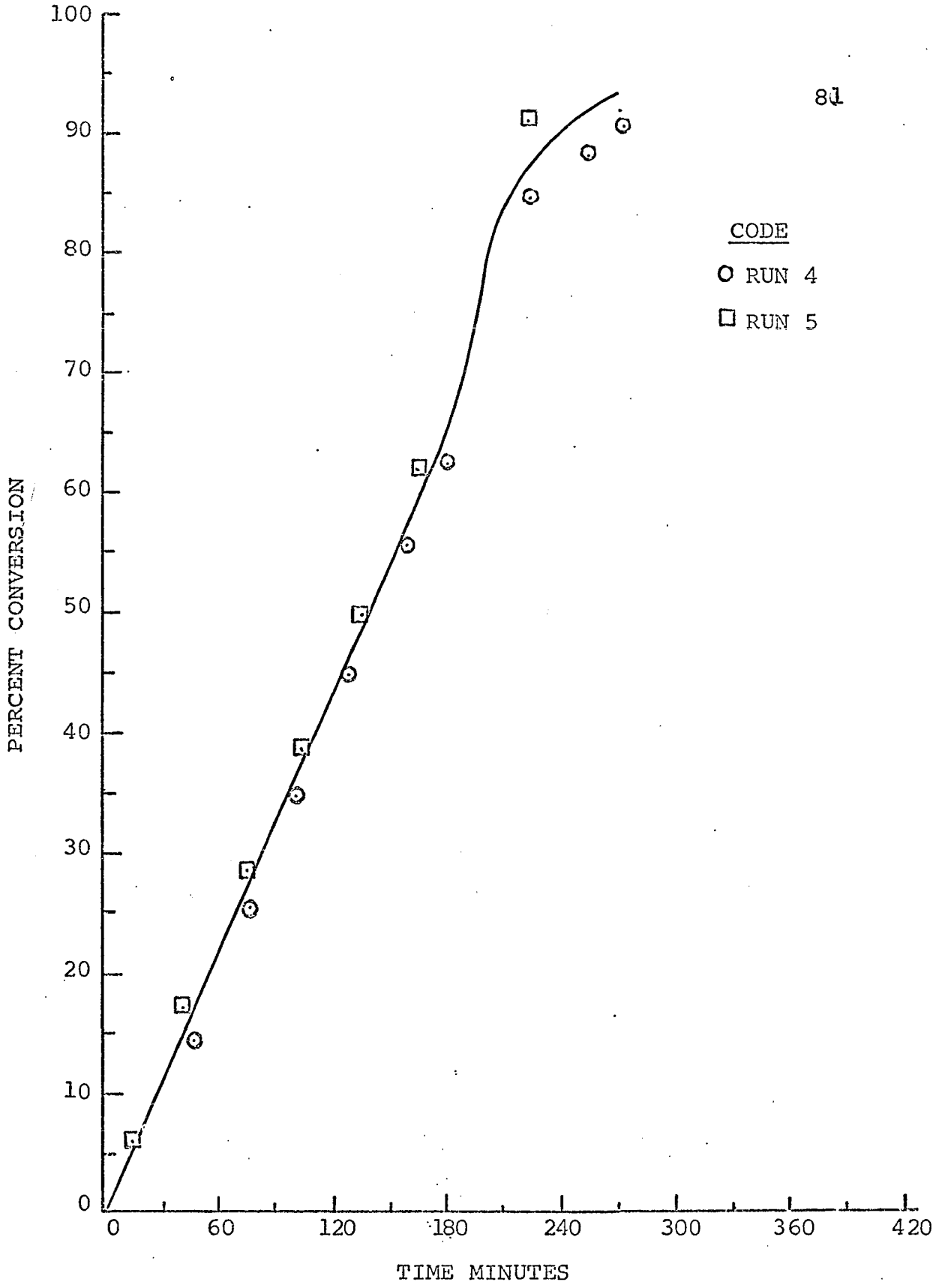

FIGURE 20 - PERCENT CONVERSION vs. TIME
DOUBLE SODIUM LAURYL SULFATE

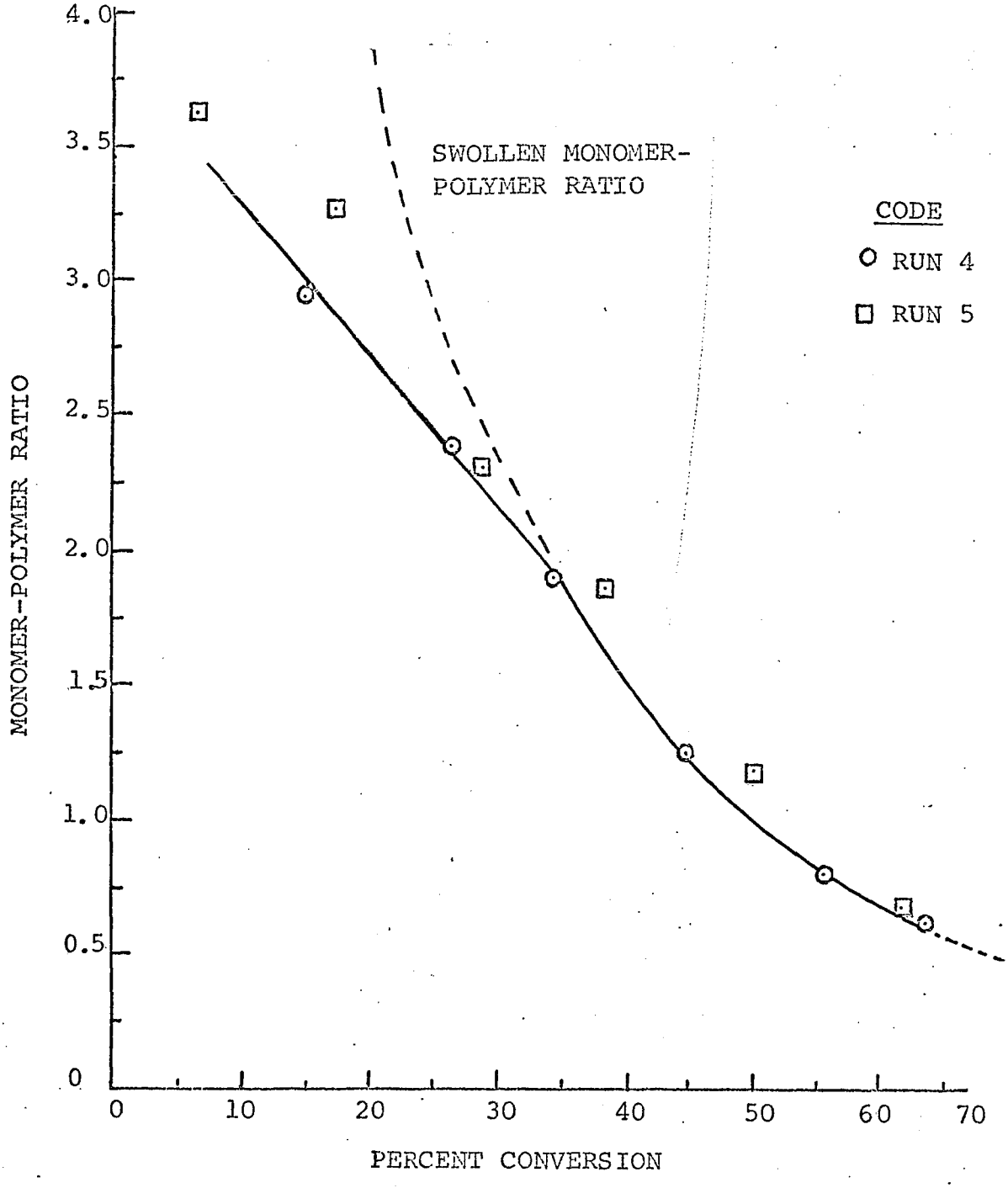

FIGURE 21 - MONOMER-POLYMER RATIO
DOUBLE SODIUM LAURYL SULFATE
CONVERSION = 21%/HR.

FIGURE 22

MONOMER-POLYMER RATIO AND CONVERSION

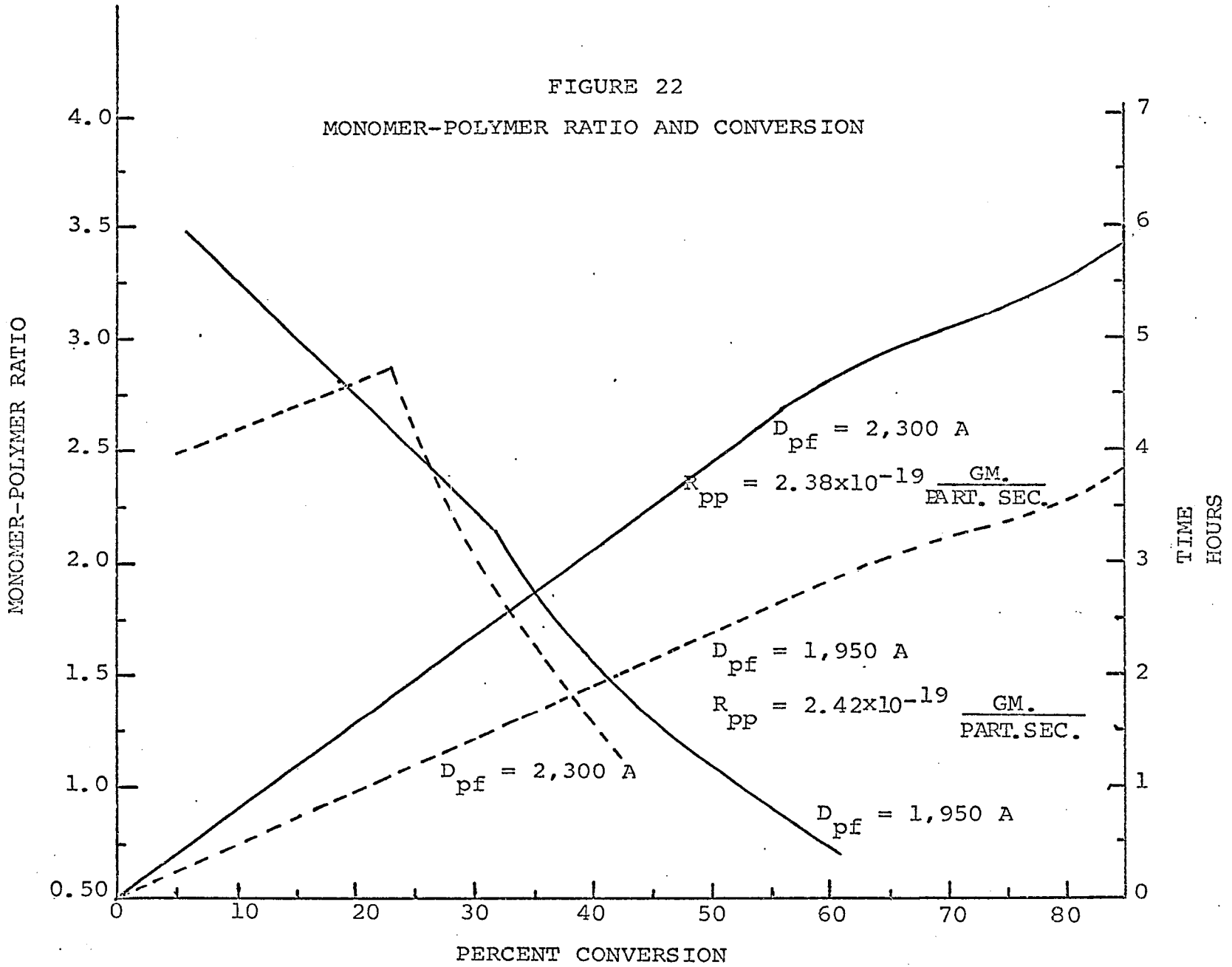

G - Rates per Particle

Since the latices studied were continuously uniform, rates per particle, R_{pp}, can be calculated by dividing the bulk rates, R_p, by the number of particles, N_p. The number of particles can be determined by dividing the initial weight of monomer, W_{Mo}, by the final weight of a single particle, W_{pf}. W_{pf} is determined from the density of polystyrene, ρ, and the final particle diameter D_{pf}. Thus:

$$R_{pp} = R_p / N_p$$

and

$$N_p = \frac{6\, W_{Mo}}{\rho \pi D_{pf}^3}$$

The results of this calculation for the two rates under consideration are given in Table 11.

TABLE 11

Rates Per Particle

R_p gms./hr.	D_{pf} A	N_p	R_{pp}, gms./part. sec.
13	2,300	1.49×10^{16}	2.42×10^{-19}
21	1,950	2.46×10^{16}	2.38×10^{-19}

In Table 11 the rates per particle for both formulations are seen to be identical. This is especially interesting when taken in conjunction with Figure 23 which shows that the monomer-polymer ratio behavior for the two runs (especially in the range from 0 - 30%C) is significantly different. This is further evidence for the fact that the polymerization rate does not depend upon the monomer-polymer ratio.

H - Summary of Kinetic Studies for Standard Formulation

1 - The latex generated by the standard formulation is continuously uniform so that attention can be focused on the individual monomer-polymer particles as the loci of reaction.

2 - Conversion behavior from 0-60%C is ideal; the conversion rate is constant with $\bar{n} = \frac{1}{2}$ and constant.

3 - Molecular weight increases several fold during the ideal period.

4 - The increase in molecular weight cannot be explained by current steady state theory, or by aqueous phenomena associated with the initiator or generated free radicals.

5 - The monomer-polymer ratio is continuously variable (changing by as much as 300%) during the constant rate period; thus, the rate of polymerization is independent of the monomer-polymer ratio.

6 - Both molecular weight development and monomer-polymer ratio show two regions of behavior during the ideal period.

7 - The polymerization rates per particle for the two formulations studied were identical.

8 - New experimental techniques are presented and the scatter in the data is at least an order of magnitude smaller than the trends being discussed.

IV - Presentation and Discussion of a Model

A - Introduction

In this section a heterogeneous monomer-polymer particle model is presented that is consistent with the results of the present study as well as the data in the literature. The discussion follows along four lines. First, the model is suggested by a consideration of the accumulated kinetic data. Second, the physical ramifications of the model are discussed. Third, a direct experimental confirmation of the model is presented, and finally, the model is extended to explain the observed molecular weight development. Although the model to be described is mainly based on the one system studied, it should be noted that this system is typical of many normally encountered in emulsion polymerization.

B - Kinetic Analysis

The rate of polymerization per particle in emulsion polymerization is expressed as:

$$(14) \quad R_{pp} = k_p \bar{n} [M]$$

where k_p is a specific rate constant. The data coupled with equation (14) suggest a heterogeneous monomer-polymer particle according to the following rationale:

In this study, R_{pp} has been measured as constant, and $\bar{n}$ has been determined to be constant and equal to ½ up to 60 percent conversion. Since the overall particle monomer-polymer ratio changes 300% during this period, equation (14)

suggests that the bulk of the polymerization occurs in a zone of constant monomer concentration within the particle. Specifically, it is proposed that the monomer-polymer particle consists of a polymer rich core surrounded by a monomer rich shell. Polymerization takes place at the core surface so that the particle grows in an onion skin manner. A radical enters and polymerizes around the core in a monomer rich environment until another enters to terminate it; the particle then lies dormant until the next radical enters. This interpretation changes the physical concept of the monomer-polymer particle but preserves the basic tenets of Smith-Ewart theory.

By using the model presented we should be able to calculate polymerization rates per particle by using equation (14) with a rate constant determined via bulk polymerization, an experimentally determined $\bar{n}$, and a monomer concentration equal to the density of pure monomer. The density of pure styrene is 905 gms./l and for the system of interest, $\bar{n} = \frac{1}{2} \times \frac{1}{6.02 \times 10^{23}} \frac{\text{moles}}{\text{particle}}$. The most recent determination of k_p in styrene polymerization is reported by Olive et al. (41) as $\log k_p = 6.340 - 1295/T$ where k_p has units of l/mole sec. and T is in $^{\circ}K$. Thus, at $60^{\circ}C$ $k_p = 282$ l/mole sec. and by equation 14, $R_{pp} = 2.12 \times 10^{-19}$ gm./particle second. The experimentally determined value of R_{pp}, it will be recalled, was 2.40×10^{-19} gm./particle second. The rather good agreement

between the two independently determined values offers strong support for the model.

C - Physical Considerations

Before presenting direct evidence for the existence of the model it might be appropriate at this point to discuss some of the physical aspects of the model. To begin, the fact that styrene monomer is slightly soluble in water [0.2 gm./l at 60°C (27)] while polystyrene is essentially insoluble in water suggests itself as a likely driving force for the particle configuration suggested. The monomer shell provides a buffer zone between the polymer and water, and repulsion between a growing chain radical and the aqueous phase drives an entering radical to the polymer core thus accounting for polymerization around the core.

Particle nucleation studies by Williams (16) and Roe (17) further suggest that monomer-polymer particles are generated by polymer chains precipitated in the aqueous phase at early conversions rather than from soap micelles. Williams did not observe particles below 5 percent conversion or less than 500 A in diameter (500 A, as will be discussed below, is on the order of the expected radius of a randomly coiled polymer chain) while Roe observed emulsion polymerization in systems where the original soap concentration was well below the critical micellar concentration.

A consideration of the relative sizes of the monomer-polymer particle and a polymer chain is important in understanding the morphology of the monomer-polymer particle. Figures 2-5 indicated that the particle diameter ranges between 1,000 and 2,300 A as conversion increases from 8% to 100%. Again, it was shown that the cumulative number average molecular weight increased from 100,000 to over 500,000 between 0 and 60% conversion and that all samples studied by GPC contained small fractions of polymer as high as 15,000,000 in molecular weight. A polystyrene molecule of molecular weight 500,000 would have an extended chain length of about 12,500 A in the zig zag conformation and a radius of gyration, R_G, of 295 A (in a good solvent) in the random coil conformation (31). Since the radius of a sphere is 2.45 times the radius of gyration this would imply a spherical coil diameter equal to about 1500 A. Therefore, an individual chain in solution would normally pervade a volume as large or larger than the monomer-polymer particle itself and would have an extended chain length five to six times greater than the particle diameter. It can also be shown that by 10 percent conversion each particle may already contain as many as 1,000 chains. Each of these chains contains bulky benzene ring side groups, and yet they are all packed within a space normally pervaded by a single molecule. Growth around the polymer core provides a reasonable explanation for such efficient packing. The packing of a large number of molecules into a relatively small volume should in-

troduce a crowding force that would tend to cause particle expansion. This force is not accounted for in the normal energy treatment of the monomer-polymer particle (15). The fact that the polymer core does not expand could be explained by the polymer-water repulsion force.

D - Direct Confirmation of the Model

The following experiment was performed as a direct test of the model (see Appendix G for details). Butadiene was added to a styrene latex at 20 percent conversion and the latex was carried to 100 percent conversion. Butadiene copolymerizes with styrene leaving residual double bonds. The residual double bonds were reacted with Osmium Tetraoxide thereby "staining" the double bonds. The particle was imbedded in Epon and then microtomed or sliced and viewed in cross section under an electron microscope. Because of the difference in electron opacity between the stained double bonds and the unstained polymer, any section of the particle containing reacted butadiene would appear darker. If the model described were correct the sample would show an unstained central core representing the polystyrene formed before the addition of butadiene. If the particle were homogeneous at all times the butadiene would permeate the entire particle when added and the stain would be observed throughout the particle.

Figure 23, which is an electron micrograph of a single particle treated as described, does indeed show the

unstained central core surrounded by the stained shell which formed after the addition of butadiene. This micrograph is presented as direct verification of the model proposed on the strength of the kinetic analysis. In Figure 23 the spherical nature of the particle has been distorted somewhat in the process of microtoming. It is suggested here that the microtoming technique be perfected and that the experiments described be extended.

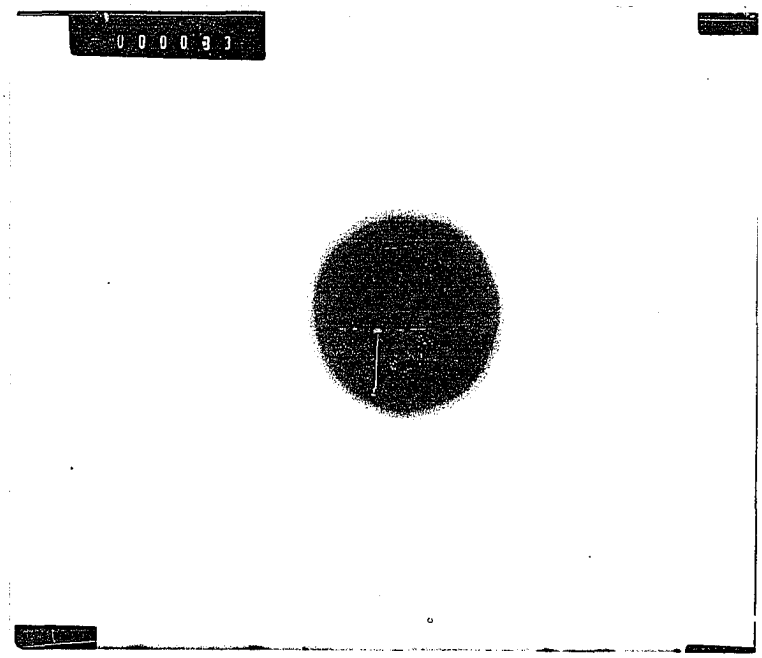

Figure 23: ELECTRON MICROGRAPH OF A HETEROGENEOUS MONOMER-POLYMER PARTICLE - MAGNIFICATION 125,000 X BUTADIENE ADDED TO STANDARD FORMULATION AFTER 20%C. SAMPLE IMBEDDED IN EPON AND STAINED WITH OSMIUM TETRAOXIDE.

E - Molecular Weight Development

The heterogeneous particle model can be further extended to explain molecular weight development during the ideal period by including a mechanism for the loss of a portion of short chain radicals by migration into the polymer core. A radical entering a monomer-polymer particle would be driven toward the polymer core because of repulsion between it and the aqueous phase. The passage of any individual chain could be more or less direct. If migration to the core were rapid, the resulting short chain radicals could readily enter the core. These "lost" radicals would not effect termination of a radical already present in an active particle and would contribute negligibly to the polymerization rate because of the monomer starved condition of the core. Thus they would have relatively little effect on the polymerization mechanism. On the other hand, if migration to the core happened to be more indirect, the resulting longer chain radical, because of its size, would not be as likely to enter the core and it would terminate a radical already growing within a particle almost instantaneously. If the particle were inactive the longer chain radical would initiate polymerization upon reaching the core surface.

The probability of loss by migration into the polymer core would increase with core size, allowing for prolonged growth of existing radicals and thus accounting for the observed molecular weight increase. Initially, with

zero core size none of the radicals are lost, and the zero time correspondence of observed and predicted molecular weights is explained. In the early conversion range, 0-30%, the core volume is increasing at a relatively rapid rate (for example core volume triples between 10 and 30%C), and the ratio of observed to predicted molecular weight increases sharply (Table 3). Between 30 and 60 percent conversion the ratio does not change much indicating that the increase in core volume in this range does not appreciably increase the probability that short chain radicals will be captured. Beyond 60 percent conversion more than one radical at a time is present in a particle and the observed molecular weight decreases.

An early paper by Kolthoff et al. (30) lends independent support for the existence of "lost" radicals. In their persulfate tracer studies with the mutual recipe, they found that small amounts of short chained, water extractable alkyl sulfates had formed and that the number of polymeric sulfate chain ends (determined with the aid of viscosity average molecular weight) for the pure polymer was greater than 2 and as high as 3.1. Kolthoff et al. could not explain their results, but it is suggested here that these materials reflect the existence of "lost" radicals. If this were the case, the extra sulfate count could be explained in terms of trapped-radical-produced alkyl sulfates which were too high in molecular weight to be water extractable but too low to affect the viscosity average molecular weight measurements.

A direct confirmation of the molecular weight development aspects of the model would involve pinpointing the location of the proposed short chain radicals trapped in the polymer core and then quantitatively determining them. Selective precipitation, washing, and/or chromatography are suggested as starting points in the experimental location of the radicals and the development of a spectroscopic technique is suggested for the quantitative determination.

V - Appendix

A - Polymerization

1 - Treatment of Materials

Dow styrene monomer at inhibitor (hydroquinone) level 12T was purified by vacuum distillation, washed with caustic to remove all traces of inhibitor and stored at -10°C until used. Immediately before use, the styrene was nitrogen purged for 30 minutes to remove oxygen which inhibits the polymerization reaction.

Water was distilled and boiled vigorously for 30 minutes before use to remove oxygen.

Samples of Triton X100 containing 98% active ingredient were obtained from Rohm and Haas and used directly. Triton x100 is a non-ionic octylphenoxyethanol surface active agent with the structural formula:

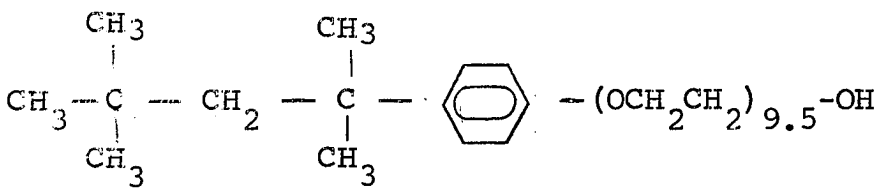

All other materials used were reagent grade chemicals of at least 98% purity.

2 - Reactors Employed

Kettle Reactor - The kettle reactor was charged as follows: 0.1500 ± .0005 gms. of sodium lauryl sulfate and 0.0750 ± .0050 gms. of KOH were weighed directly into a 1 liter kettle. 3.00 ± .01 gms. of Triton x100 was weighed into an aluminum dish which was added to the kettle. 160 gms. of water were added hot (80°C) and 100 gms. of styrene cold (room temperature). The formulation was stirred in the kettle and the aluminum dish removed. The kettle was then fitted with a condenser, thermometer, teflon paddled glass stirer and a glass tube bent at an angle of about 60°. The condenser and stirring apparatus were equipped with standard taper 24-40 joints. The thermometer and glass tube were sealed into the kettle by means of gasketed standard taper 24-40 teflon plugs. The kettle was clamped in a ring stand and submerged in an oil bath. The mixture was heated to 60 ± 1°C while being nitrogen purged and agitated for 30 minutes or more. A preheated solution of 0.500 gms. of $K_2S_2O_8$ in 20 ml. of water was then added to the kettle by pipette. The $K_2S_2O_8$ solution was prepared as 5.0000 ± 0.0005 gm. $K_2S_2O_8$ in 200 ± 1 ml. of water. At this point the reaction was considered to have started and the temperature was maintained at 60 ± 1°C without the aid of cooling devices. Nitrogen (at 1 psig) was passed into the glass tube which reached to within 1/4" of the bottom of the reactor, bubbled through the reacting emulsion and exhausted through the condenser to maintain an oxygen free

atmosphere. When it was desired to withdraw a sample, the nitrogen gas flow was diverted through the condenser. This forced a sample of the reacting emulsion up through the glass tube where a sample could be collected in a vial. A system of 3 way stopcocks was used to change the direction of nitrogen flow without admitting air into the system. This sampling technique caused a minimal disturbance to the reaction.

Although agitation was not studied explicitly it was found to be a very important factor. At very low agitation, conversion rates were low and not reproducible while at very high agitation various degrees of coagulation were observed at conversions greater than 40%. Thus an intermediate stirring rate was used: about 100 rpm with a one inch anchor type teflon paddle.

Bottle Polymerizer - A bottle polymerizer was designed and built with the aid of the Chemical Engineering Shop. The bottle polymerizer essentially consists of a covered stainless steel tank, 40 inches long by 25 inches wide by by 30 inches deep, filled to a depth of 24 inches with water and insulated with asbestos board, plywood, and canvas. The water is heated to a given temperature by means of two six-kilowatt Chromalox heaters. Temperature control is effected by means of an on-off relay system connecting a temperature sensing element to the heaters.

The reactor bottles were held in cylindrical clamps which were soldered to wheels that rotated while submerged in the constant temperature water-bath. Specifically, the bottles were located on centers eight inches from the common axle of the wheels and tumbled end over end while the temperature was maintained at 60 $\pm$ 0.5°C. There were three wheels in the bath for a total accommodation of twelve bottles. The wheels were driven at 30 rpm by a single speed motor. It is suggested that a variable speed motor be attached to the tank for greater flexibility in future use.

The bottles were standard 12-ounce "soda-pop" bottles purchased from the "Goodo" Beverage Company. Three 1/16 inch holes were punched in the fitted crown caps used to seal the bottles. The bottles were always filled to an approximate total volume of 300 ml. It was found that for the standard formulation, tank design, rpm, bottles, and pressures used in these experiments, any lesser volume gave rise to agitation sufficient to cause serious coagulation within the bottle. It was further important to fill the bottles to approximately the same level for every run so that dynamic equivalence would be maintained between runs. Sealing was effected with a laminated rubber gasket consisting of circles of hard rubber and butyl-sealant rubber.*

*Designated as "w-7" and "w-9" rubber respectively and obtainable from B.F.Goodrich Co., Research Center, Brecksville, Ohio

The circles were cut so that the hard rubber one fit just inside the cap and the butyl-sealant one fit just inside the bottle opening. These were cemented together with Eastmann 910 adhesive and placed inside the cap so that the smaller circle faced and covered the holes in the caps. After the caps had been pressed on, a few drops of toluene were placed over the holes in the cap causing the butyl-sealant rubber to swell and effect a tight seal. Materials could be added to or removed from the sealed bottles with hypodermic syringes and needles. Twenty gauge 1½ inch Luer Lock Huber point needles were used.

The formulation was charged to cleaned, oven dried bottles in liquid form so a master batch solution of sodium lauryl sulfate, Triton X100 and KOH was made for each run. Most of each charge was metered in volumetrically to a rough approximation somewhat less than that actually required. A final adjustment was made gravimetrically by eye dropper addition. The Sauter Ultra-Radial Balance, No. 722, which weighed accurately to $\pm$ 0.01 gm., was used for weighing. The materials were weighed into the bottles by adding the weight of each successive charge to the weight of the bottles plus ingredients. The material was then added to make up the proper weight. The bottles were then capped, nitrogen purged for 10 minutes, and pressured with nitrogen to 10 psig. Pressuring and purging were accomplished by attaching a 7½ inch needle and hose to a nitrogen source regulated to 10 psig and then admitting nitrogen by injecting the needle into the bottle. For purging a second

needle was inserted to provide a nitrogen outlet; for pressuring the second needle was removed. $K_2S_2O_8$ was injected into the bottle with a 10 ml. hypodermic syringe just before the bottle was placed in the bottle polymerizer. A five minute induction period was observed while the bottles were being heated to 60°C.

3 - Reproducibility Between Runs

The difficulty in exactly reproducing conditions between runs was mentioned several times in the text of this dissertation. Any slight change in the number of particles formed at the start of reaction would cause a definite, measurable change in such variables as conversion rate, and molecular weight, and might influence monomer-polymer ratios. The particle nucleation phenomena is not well understood in general and is not at all known in soap starved systems. Thus, one cannot predict in advance exactly how much a slight change in initial conditions will affect particle nucleation. It is recommended here that a fundamental study of particle nucleation is necessary to achieve absolute reproducibility between runs. This is especially true because of the large number of system variables.

Consider the possible sources of error in this experiment that can lead to a change in the number of particles nucleated. (1) There is always some error in weighing ingredients (soaps, KOH, water, styrene, initiator). (2) All of the chemicals contain some impurity; this is

even true of singly distilled water. (3) There is a slight fluctuation in initial temperatures, pH, and agitation rates from run to run. (4) Even in bottle runs where bottles are filled from master batches and temperature, pH, and agitation rate should be the same for each bottle, some error is observed. This indicates the possible influence of a thus far undetected variable.

B - Electron Microscopy

Samples for particle size analysis were withdrawn from a run in progress, quenched in a .3% solution of airated hydroquinone, and diluted several times. Standard particles* were added to the sample and the sample was placed on a collodian film deposited on a nickel grid. The grid was then washed several times with hot water, and a film of platinum was deposited by vacuum evaporation to reinforce the film and shadow the particle samples.

The samples were viewed with a Norelco 300 EM electron microscope at magnifications between 18,000 and 35,000. Particle diameters were determined to within $\pm$ 50 A with a Bausch and Lomb measuring magnifier.

*Particle size standards were obtained from Dow Chemical Company - Midland, Michigan.

C - Conversion Rate

Conversion samples of approximately 5 gms. were taken from a run in progress and immediately weighed to the nearest 0.01 gm. in an aluminum dish on an analytic balance. The reaction was stopped by addition of hydroquinone solution and the sample was evaporated at 160°C. The residue was weighed to the nearest ± 0.0005 gm. If S is the weight of the sample and R the weight of the residue, conversion was determined by:

$$(A\text{-}1) \qquad \%C = 283\ R/S - 3$$

where the constant 3 accounts for Triton X100 which is not evaporated and therefore present in the final residue. The expected error and reproducibility were found to be within ± 1%. As discussed earlier the gravimetrically determined conversions agreed well with those determined by comparing the cubes of intermediate to final particle diameters.

In the inhibitor studies samples were withdrawn and inhibitor solution was subsequently added to the kettle. Thus, equation (A-1) had to be altered to determine conversions after inhibitor was added. To make this adjustment each total sample taken before the addition of inhibitor had to be weighed very carefully.

D - Molecular Weight

1 - Polymer Recovery and Purification

Polystyrene was precipitated in granular form from the latex in methanol acidified with sulfuric acid. The polymer was recovered by filtration and washed repeatedly with methanol and water. Subsequently, the polystyrene was redissolved in toluene, precipitated as a fine powder, with methanol in a Waring blender, and methanol washed several times. As discussed earlier, GPC measurements showed that this procedure eliminated all polymer of molecular weight less than 6,000.

2 - Viscosity Average

The viscosity average molecular weight was calculated from the relative viscosity of dilute toluene solutions at 30°C via the one point method of Maron (36) utilizing the equations:

$$[\eta] = KM^{a} \quad \text{and}$$

$$[\eta] = \frac{\eta_{sp} + \gamma \ln \eta r}{(1 + \gamma)C}$$

where ηr is the relative viscosity, $\eta_{sp} = \eta r - 1$, and C is measured in gm/100cc. For polystyrene in toluene solution: $\gamma = 2.73$ (36), $K = 3.7 \times 10^{-4}$ and $a = 0.62$ (37)

The final combined equation is:

$$\bar{M}_v = 40{,}000 \left[\frac{\eta_{sp} + 6.28 \log \eta r}{c}\right]^{1.61}$$

Relative viscosities were determined very accurately with less than ± 0.1% deviation from the average with Cannon Ubbelode dilution viscometers. The viscometers were stored in an oven at 90°C and nitrogen purged while cooling before use to avoid contamination with water. Toluene was distilled and all solutions were vacuum filtered through fritted glass before delivery to the viscometer to remove dust. Concentrations of approximately 0.2 gm/100cc were used. Concentrations were determined gravimetrically with ± 3% standard deviation.

3 - Number Average

Samples were prepared for osmometry in the same manner as for viscometry. Data for a sample determination are presented in Table 12 and Figure 24. For the molecular weight range encountered in this study concentrations between 1 and 10 gm./l were employed. At concentrations much above 10 gm./l the relationship between π/c and c becomes non-linear. At concentrations much below 1 gm./l large errors were introduced because of the low value of the osmotic pressure.

A Hewlitt Packard Mechrolab 501 Osmometer was used

at 37°C. For the information of future operators of the instrument, it was found that: (1) Arro 300-D gel cellophane membranes worked best giving equilibration times of about 30 minutes. (2) Filtration and preheating of samples (including pure toluene reference samples) increased accuracy and instrument performance. (3) Filling the solvent chamber with boiling toluene, and degassing membranes before use greatly decreased start-up problems. (4) Samples were measured in the order of increasing concentrations so that the osmometer did not have to be rinsed between samples.

Sample Calculation:

Using the data of Table 12, π/c is determined to be 0.100 (Figure 24). For toluene at 37°C, RT = 3.03×10^4. Using the limiting law of vant Hoff,

$$\bar{M}_n = \frac{RT}{(\pi/c)c \to o} = \frac{3.03 \times 10^4}{0.100} = 303,000$$

TABLE 12

SAMPLE CALCULATION OF NUMBER AVERAGE MOLECULAR WEIGHT

Concentration g/l	1.10	2.08	4.20	8.27
Solvent Pressure (P_o)	17.045	17.045	17.045	17.045
Pressure (P)	17.180	17.330	17.725	18.925
Pressure (P)	17.175	17.325	17.745	18.925
Av. Pressure (P)	17.175	17.330	17.735	18.925
$\pi = P - P_o$	0.130	0.285	0.690	1.880
π/c	0.118	0.137	0.164	0.228

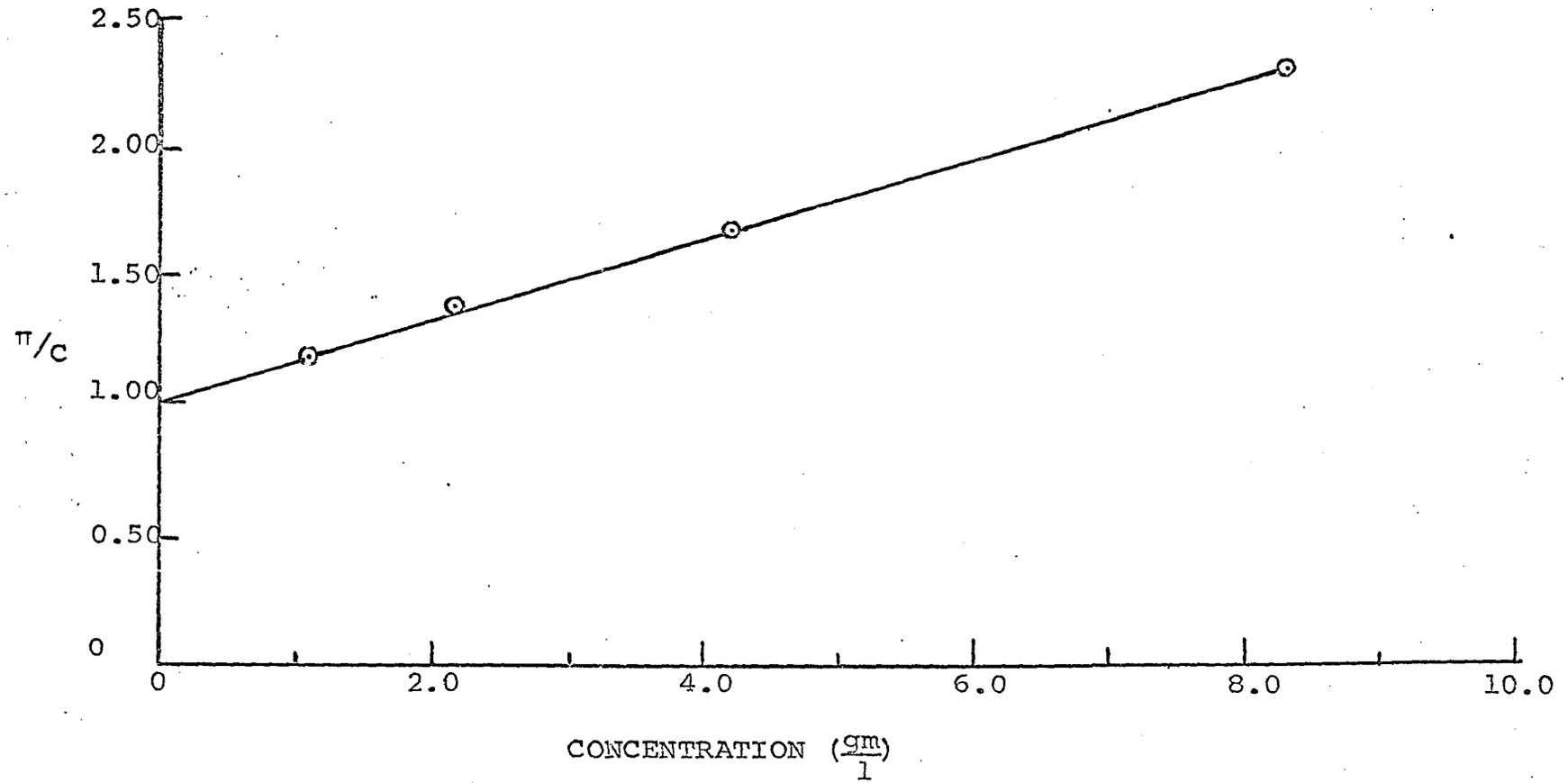

FIGURE 24. SAMPLE OSMOTOGRAPH

4 - Instantaneous Values

Instantaneous molecular weights were determined from material balances on the cumulative curves at 10% intervals. For example if the cumulative number average molecular weights at 20 and 30% conversion were measured as A and B then the instantaneous number average molecular weight being generated at 25% conversion, x, was calculated via:

$$.20\ A + .10x = .30\ B$$

Similarly if A^1 and B^1 represented the cumulative viscosity average molecular weights at 40 and 50% conversion respectively the instantaneous value at 45% conversion, x^1, was calculated by:

$$.40\ (A^1)^2 + .10\ (x^1)^2 = .50\ (B^1)^2$$

The viscosity averages were squared to weight the heavier molecules.

5 - Molecular Weight Distribution

The GPC data cannot be used extensively because of the difficulty involved in calibrating the GPC for molecular weights above 10^6. This makes accurate determination of weight fractions above 10^6 highly inaccurate.

E - Initiator Kinetics

1 - Initiator Decomposition

The details of the determination of residual persulfate were outlined in the body of the text. The procedure followed that suggested by Kolthoff (38) with minor variations such as the use of larger amounts of KI to speed the determination and omission of starch indicator. Kolthoff developed his technique for pure aqueous solutions. In this study, however, we were interested in determining residual persulfate in aqueous soap solution. The fact that the presence of the soaps did not significantly alter the validity of the titrations was substantiated by the following experiment: Three samples of 0.5 gms. $K_2S_2O_8$ in 180 ml. water were prepared. Three other samples were prepared with 0.5 gms. $K_2S_2O_8$, 0.15 gm. sodium lauryl sulfate and 3.00 gm. Triton x100 in 180 ml. water. Both sets of samples were then immediately titrated with sodium thiosulfate before the persulfate could decompose. The first set of samples required 37.0, 36.8, and 36.6 ml. of sodium thiosulfate while the second set required 37.4, 37.5, and 36.2 ml. Thus, the soaps did not alter the results of the titration.

It was found, however, that if samples containing soap were agitated, as was the case in determining decomposition kinetics, the soap foamed, making titration difficult and introducing scatter in the data. Although the scatter was small compared to the trends investigated

in this particular experiment, it is suggested that future workers in this area investigate the use of antifoaming agents to reduce the scatter.

The chemistry of the determination (38) is presented below. The potassium iodide added reacts with residual persulfate to release iodine which is quantitatively determined by titration with sodium thiosulfate.

$$S_2O_8^{=} + 2I^- = 2SO_4^{=} + I_2.$$

$$I_2 + I^- = I_3^-$$

$$I_3^- + (2e) = 3I^-$$

$$2\,S_2O_3^{=} = (2e) + S_4O_6^{=}$$

$$S_2O_8^{=} + 2S_2O_3^{=} = 2SO_4^{=} + S_4O_6^{=}$$

In the actual performance of the decomposition studies the following technique was developed. A standard solution of sodium thiosulfate (0.1N) was prepared from a concentrated commercial solution (1.0N); a master batch solution of $K_2S_2O_8$ was also prepared. Five samples from the persulfate solution (at 0% decomposition) were titrated with thiosulfate and the results were averaged (standard deviation $\pm$ 3%). Samples were then prepared by adding soap to the persulfate solution. These samples were then allowed to decompose at 60°C for various times (as

described earlier) and titrated. The percent decomposition was calculated as the ratio of the quantity of thiosulfate consumed by the heated sample to the average quantity of thiosulfate consumed by the five 0% decomposition standards. It is felt that this technique decreased the possibility for error by standardizing the thiosulfate solution against the persulfate solution actually used on any given day.

2 - Inhibitor Studies

The inhibitor technique is predicated upon the fact that paraquinone will react with the free radicals being generated before they can effectively initiate polymerization. Thus, polymerization will not take place until all of the paraquinone is consumed, and an induction period is subsequently observed. If the chemistry of the radical-paraquinone reaction is known, and the induction period is accurately measured, the number of radicals generated during the induction interval can be easily determined from the amount of inhibitor added.

The application of an inhibitor technique to this study was unique in that paraquinone was added to a run already in progress. Polymerization ceased immediately upon the addition of paraquinone solution to the reacting latex; a clean induction period was observed, and eventually polymerization resumed. Although paraquinone is more water than styrene soluble a sufficient quantity entered monomer-polymer particles to stop previously activated chains within seconds.

A reaction chemistry based on the work of Price et al. (39) in which two moles of quinone are consumed for each radical captured was found to best fit the data. The proposed reaction scheme in which R• represents SO_4^-• is as follows:

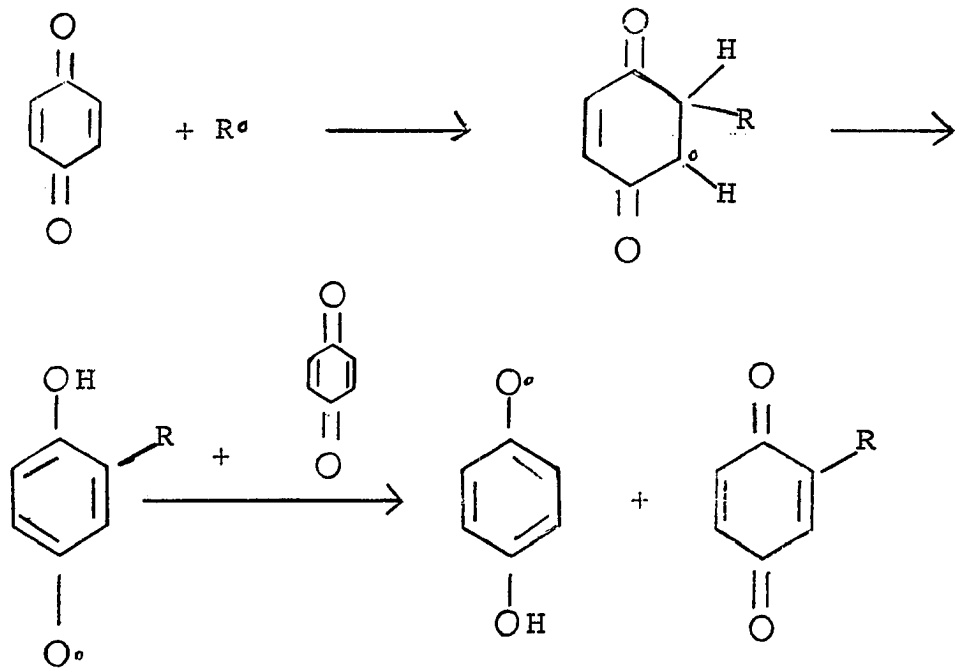

In Table 7, an adjusted induction period was determined by multiplying the observed induction period by the ratio of the observed conversion rate before the addition of paraquinone to 13.0. The reasoning behind the adjustment is as follows: As previously discussed, it was not possible to exactly reproduce rate behavior. Hence, the induction runs each exhibited slightly different initial conversion rates. It was felt that the slight variations in conversion rates should be directly associated with slight variations in the initiator decomposition kinetics, with higher rates reflecting accelerated decomposition and lower rates decelerated decompositions. So by adjusting the induction period all of the data were "corrected" to the average

decomposition kinetics which yield an average conversion rate of 13%/hr. Although the corrections are small and they do not substantially alter the arguments made, they are in a direction which "smoothes" the data. The method of correction is not exactly accurate but the corrected data are probably more meaningful than the uncorrected data.

F - Monomer-Polymer Ratio

Sampling: Samples were collected from a run in progress directly into centrifuge tubes containing paraquinone. After the styrene layer was separated by centrifugation a sample of latex (lower layer) was withdrawn by pipette and delivered to refluxing stirred THF. It was found that the samples had to be hot and well stirred before injection into the chromatograph to obtain reproducibility. Duplicate samples for each determination were injected into the chromatograph with a 10 microliter syringe. The peak height ratios of styrene to water for the duplicate samples were within ± 3% of each other.

Experiments were also performed in which the styrene layer was separated from the latex after centrifugation and the latex was diluted with an equal volume of water. The samples were then recentrifuged to determine any residual monomer retained by the latex. For all samples above 5% conversion a "second" styrene layer was not observed.

Instrument Settings: A Hewlitt Packard gas chromatograph was employed with a carbowax and teflon column. The settings were: oven: 95°C, injection port: 185°C, detector: 230°C. The bridge current was 175 ma, and the gas flow 60cc/min.

Calibration: The chromatograph was calibrated by injecting samples containing styrene, water, and THF in proportions covering the required range, (Styrene/Water ranges from 0.555 to 0), and determining the peak height ratios of styrene to water for each sample. Sample calibration curves determined on 5/68, and 11/68 are presented in Figure 25. As can be seen from the figure the calibration changed from day to day so that the chromatograph had to be calibrated on the day of use.

Calculation: The peak height ratio was transmitted into gms. styrene/gm. water, γ, by means of the calibration curve. Since there were 180 gms. of water in the original formulation 180γ represents the weight of unpolymerized styrene in monomer-polymer particles. Again, since the original formulation contained 100 gm. of styrene the quantity of polymer in the latex particle is given directly by the percent conversion, %C, which was gravimetrically determined. Thus,

$$M/_P = 180 \frac{\gamma}{\%C}$$

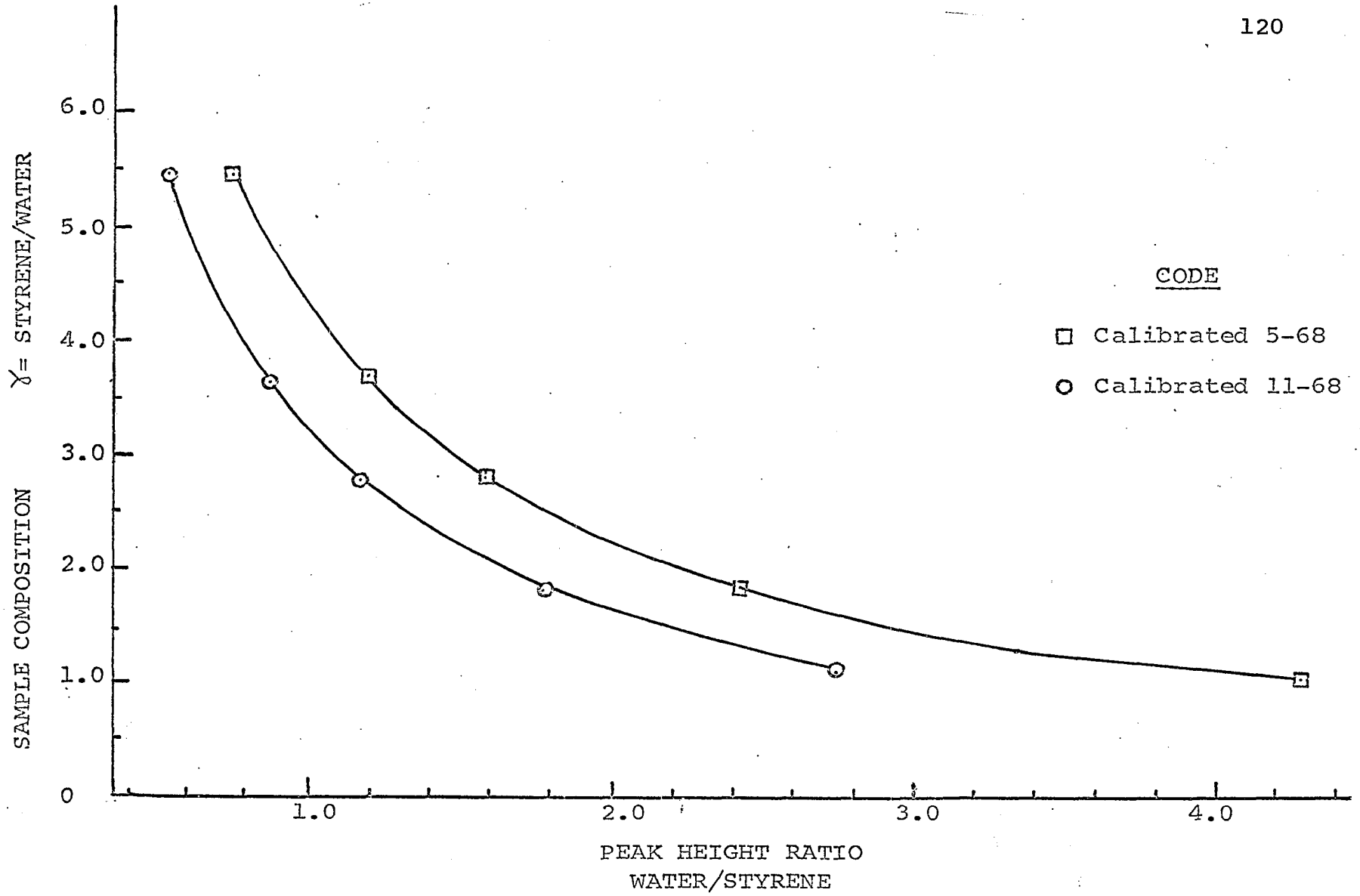

FIGURE 25. SAMPLE CHROMATOGRAPH CALIBRATION

Discussion of Errors: As mentioned earlier a slight disparity was noticed between the monomer-polymer ratio observed and that predicted from conversion data after all of the monomer was imbibed by the monomer-polymer particles. It will be remembered that the observed curves were parallel to the "predicted" curve but slightly displaced. The displacement is attributed to two possible sources of error:

(1) The calibration samples could have been slightly inaccurate. This would shift the position of the monomer-polymer ratio curve. For the 21%/hr. run two separate sets of calibration samples were used to calibrate the chromatograph before the two runs. For the 13%/hr. runs the same calibration samples were used to calibrate the chromatograph before each of the three runs; this would explain all of the data for the three runs falling on the same curve.

(2) In the 13%/hr. run latex samples were injected into refluxing THF by means of a hypodermic syringe. The shear developed in forcing the latex through the needle could cause a portion of the monomer-polymer particles to coat the needle wall resulting in a consistently low value of monomer-polymer ratio, as observed. This technique was modified in the 21%/hr. runs. It should again be stated, however, that the errors were small compared to the trends being investigated.

G - Investigation of Latex Particle Morphology

The experimental procedure used in investigating the morphology of the monomer-polymer particle was as follows: Butadiene was liquified by passing the gas through copper coils immersed in an ice-salt bath maintained at -10°C. 10 ml. of the collected butadiene along with 0.1 ml. of dodecyl mercaptain were added to the standard formulation at 20% conversion and the reaction was carried to 100% completion. The resultant latex was frozen at -10°C and dried to a crumb in air. The particles were then washed several times with methanol and water to remove soap, and again air dried.

The washed, dried particles were poured into polyethylene Beem capsules, and Epon was poured over the particles to act as an imbedding medium. The Epon was oven cured at 45°C for 48 hours. The sample containing polystyrene particles imbedded in cured Epon, was then sectioned into fine slivers on a microtome. In slicing, some of the imbedded particles were sliced through the center exposing the particle cross section. The sectioned slivers were picked up on electron microscope grids to which they adhered and placed in Petri dishes. They were then exposed to fumes of Osmium Tetraoxide which reacted with residual double bonds in the butadiene. The Osmium Tetraoxide is electron opaque so that those areas of the particle containing butadiene did not transmit electrons as well as those areas not containing butadiene. The difference in electron opacity is indicated by the

contrast in shade observed in Figure 25, which was taken through the Norelco 300 E M . electron microscope.

The microtoming and imbedding procedure was carried out by Mr. John Bodnaruk who worked in conjunction with the Biology Department of The City University of New York.

Bibliography

1. Harkins, W.D., J. Amer. Chem. Soc., 69, 1428 (1947).
2. Smith, W.V., and Ewart, R.H., J. Chem. Phys., 16, 592 (1948).
3. Stockmayer, W.H., J. Polymer Science, 24, 314 (1957).
4. Otoole, J.T., J. App. Polymer Sci., 9, 1291 (1965).
5. Smith, W.V., J. Amer. Chem. Soc., 70, 3695 (1948).
6. Smith, W.V., J. Amer. Chem. Soc., 71, 4077 (1949).
7. Brodnyan, J.G., Cala, J.A., Konen, T., Kelley, E.L., J. Coll. Sci., 18, n1, 73 (1963).
8. Kolthoff, I.M., Meehan, E.J. and Carr, E.M., J. Amer. Chem. Soc., 75, 1479 (1953).
9. Gerrens, H., Agnew Chem., 71, n19, 608 (1959).
10. Gerrens, H., Z. Elektrochem., 60, n4, 400 (1956).
11. Williams, D.J., and Bobalek, E.G., J. Polymer Sci., Part A-1, 4, 3065 (1966).
12. Gardon, J.D., J. Polymer Sci., Part A-1, 6, 687 (1968).
13. Saidel, G. and Katz, S., Polymer Preprints, A.C.S. Division of Polymer Chem. 6, 737 (1966).
14. Van der Hoff, B.M.E., "Polymerization and Polycondensation Processes," Advances in Chem. Series, n34, (1962), Amer. Chem. Soc., Washington, D.C.
15. Morton, M., Kaizerman, S., and Altier, M.W., J. Chem. Soc., 9, 300, (1954).
16. Williams, D.J., Ph.D. Thesis, Case Institute of Technology, (1964).
17. Roe, C.B., Ind. and Eng. Chem., 60, n9, (1968).
18. Medvedev, S.S., International Symp. on Macromol. Chem., Pergamon Press, New York (1959) p. 174.
19. Gardon, J.D., J. Polymer Sci., Part A-1, 6, 623, (1968).

20. Gardon, J.D., ibid., 6, 643, (1968).

21. Gardon, J.D., ibid., 6, 665, (1968).

22. Gardon, J.D., ibid., 6, 2853, (1968).

23. Gardon, J.D., ibid., 6, 2859 (1968).

24. Herzfield, S.H., Roginsky, A., Corrin, M.L. and Harkins, W.D., J. Polymer Sci., 5, 207, (1950).

25. Bovey, F.A., "Emulsion Polymerization," Interscience Pub. Co., New York, (1955).

26. Meehan, E.J., J. Amer. Chem. Soc., 71, 628 (1949).

27. Vanzo, E., Marchessault, R.H. and Stannett, V., J. Chem. Soc., 20, 62 (1965).

28. Kolthoff, I.M., and Miller, I.K., J. Amer. Chem. Soc., 73, 3055, (51).

29. van der Hoff, B.M.E., J. Polymer Sci., 44, 241 (1960).

30. Kolthoff, I.M., O'Connor, P.R., and Hansen, J.L., J. Polymer Sci., 15, 459 (1955).

31. Tanford, C., "Physical Chemistry of Macromolecules," John Wiley and Sons, New York (1961) p. 306.

32. Loranger, A.H., Serafini, T.T., Von Fischer, W. and Bobalek, E.G., Off. Dig. Federation Paint Varnish Production Clubs, 31, n44, 482 (1959).

33. Serafini, T.T., and Bobalek, E.G., Off. Dig. Federation Paint Varnish Production Clubs, 32, n10, 1259 (1960).

34. Woods, M.E., Private Communication, Case Institute of Technology.

35. Maron, S.H., Moore, C. and Powell, A.S., J. Appl. Phys., 23, 900 (1952).

36. Maron, S.H., J. Appl. Polymer Sci., 5, 282 (1961).

37. Goldberg, A.I., Hohenstein, W.P. and March, H., J. Polymer Sci., 2, 503 (1947).

38. Kolthoff, I.M., and Carr, E.M., Analytical Chem. 25, n2, 298 (1955).

39. Price, C.C. and Read, D.H., J. Polymer Sci., 1, 44 (1946).

40. Krackeler, J.J., and Naidus, H., Polymer Preprints A.C.S. Division of Polymer Chem. 6, 791, (1966).

41. Olive-Henrici, G. and Olive, S., Makromol. Chem., 37, 71 (1960) German.

VITA

Michael R. Grancio was born in Brooklyn, New York on April 24, 1942. He received his elementary and secondary education in the New York City School System. He entered The City College of New York in September of 1959 and received his Bachelor's degree in Chemical Engineering in February 1964.

From February to September of 1964 he was employed by Interchemical Company as a Research Engineer. In September 1964 he returned to The City University of New York for full time graduate studies, and was supported, in chronological order, by a Research Assistantship, a National Science Foundation Graduate Traineeship and an NSF grant awarded to Dr. David J. Williams. As a result of his graduate research he has coauthored three papers with Dr. Williams.

Michael R. Grancio is currently employed by the Monsanto Company as a Senior Research Engineer in the Fundamentals Section of the Research Department in Springfield, Massachusetts. He resides in Fairview, Massachusetts with his wife Susan.